A Middle Miocene vertebrate assemblage from the Vienna Basin of the southern Czech Republic: implications for the paleoenvironments of the Central Paratethys

Jakub Březina[a,b,*], David M. Alba[c], Martin Ivanov[b], Martin Hanáček[d], Àngel H. Luján[b,c]

[a] *Department of Geology and Paleontology, Moravian Museum, Zelný trh 6, 659 37 Brno, Czech Republic*

[b] *Department of Geological Sciences, Faculty of Science, Masaryk University, Kotlářská 2, 611 37 Brno, Czech Republic*

[c] *Institut Català de Paleontologia Miquel Crusafont, Universitat Autònoma de Barcelona, Edifici ICTA-ICP, c/ Columnes s/n, Campus de la Universitat Autònoma de Barcelona, E-08193 Cerdanyola del Vallès, Barcelona, Spain*

[d] *Department of Geography, Faculty of Science, Masaryk University, Kotlářská 2, 611 37 Brno, Czech Republic*

* Corresponding author

E-mail addressess: jbrezina@mzm.cz (J. Březina), david.alba@icp.cat (D.M. Alba), mivanov@sci.muni.cz (M. Ivanov), HanacekM@seznam.cz (M. Hanáček), angel.lujan@icp.cat (À.H. Luján)

Abstract

      Czujan's sandpit is an abandoned quarry in the Vienna Basin (Mikulov, Czech Republic) that has yielded an important middle Miocene vertebrate assemblage. Here we re-describe the site from the perspective of sedimentology, taphonomy, and paleoenvironments, and further review the biochronology of the fauna to clarify the age. The updated faunal list includes two testudines (one trionychid and one medium-sized testudinid), and 12 species of terrestrial mammals (three proboscideans, four perissodactyls, four artiodactyls, and one carnivoran), consistent with an early Astaracian (MN6) age. The position of the Wielician/Kosovian boundary just below the floor of Czujan's sandpit, and our new biostratigraphic data, further allow us to constrain the fossil assemblage to the latest MN6 (late Badenian, ~13.6 Ma) and resolves a longstanding controversy about the age of the site. The site exposes a coarsening-upward succession deposited in a braid delta environment, and comprises three facies association: from bottom to top, pelagic sediments (FA1); prodelta and delta slope sediments (FA2); and distributory channel infills of the delta front and delta plain (FA3), the latter containing all the studied terrestrial vertebrates. We propose two taphonomic explanations for the genesis of the vertebrate assemblage: (1) a time-averaged assemblage generated by riverine transport, or (2) a transported assemblage from a mass death site(s), with mass death episode(s) caused by seasonal droughts in the river catchment. Our new findings allow the more precise reconstruction of late Badenian terrestrial paleoenvironments in the northwest area of the Vienna Basin and adjacent Carpathian Foredeep Basin. This region comprised a mosaic of continental habitats dominated by woodlands but also including forest patches and more open environments.

48

1. Introduction

The intramontane Vienna Basin is among the best explored Paratethyan basins, where decades of research of both marine and brackish sedimentary deposits have greatly contributed to the understanding of paleoenvironmental changes during the middle to late Miocene (e.g., Jiříček, 2002; Kováč et al., 2007, 2018; Harzhauser et al., 2011, 2018). Paleoenvironmental reconstructions of the middle Miocene environment are largely based on the marine fauna (e.g., Harzhauser et al., 2011) or palynoflora (e.g., Kvaček et al., 2006; Kováčová et al., 2011; Kovar-Eder and Teodoridis, 2018). Middle Miocene sites with terrestrial vertebrates are rather scarce with only two well-documented localities, comprising Klein-hadersdorf, Austria (e.g., Thenius, 1948, 1951; Böhme et al., 2012) situated close to the studied site in western part of the Vienna Basin; and Devínska Nová Ves, Slovakia (e.g., Zapfe, 1949, 1954, 1979, 1993; Estes, 1969; Sabol and Holec, 2002; Sabol and Kováč, 2006) situated at the southeastern margin of the Vienna Basin. A detailed paleoenvironmental analysis based on the complete spectrum of the terrestrial taphocoenosis has been conducted only for the Devínska Nová Ves-"Bonanza" site (Sabol and Kováč, 2006).

Here we revise the evidence from another, less known, vertebrate site called Czujan's sandpit (sand quarry), which is situated close to the Carpathian Foredeep Basin at the northwestern margin of the Vienna Basin (Fig. 1). This site has yielded a high concentration of fossil macrovertebrates. However, this relatively diverse assemblage has remained largely unpublished, even though it constitutes one of the most important middle Miocene mammal assemblages from the Central Paratethys. The importance of this site increased in the 1950s, when Thenius (1951) established it as a type locality of the bovid *Tethytragus stehlini*. Later, the description of the proboscidean fauna (Holec, 1985; Seitl, 1985) highlighted this locality as one of the most important occurrences of the relatively rare proboscidean *Zygolophodon*

73   *turicensis*. Despite the significance of the studied site, the fossil fauna, its taphonomy and

74   sedimentology has never been studied comprehensively. Accordingly, the research carried out

75   since the 1930s did not provide a clear agreement on the stratigraphical position of this site

76   (e.g., Seitl, 1985; Čtyroký et al., 1990; Stráník et al., 1999). Moreover, Late Miocene

77   mammals are known from other abandoned sandpits (Fig. 1B) in the southern area of Mikulov

78   as well. Although multiple sites near Mikulov have been grouped as a single locality, Mikulov

79   (= Nikolsburg), and considered contemporaneous (e.g., Abel, 1910; Rzehak, 1922; Stejskal,

80   1934; Thenius, 1959; Fejfar, 1990; Böhme et al., 2012), Middle and Late Miocene vertebrates

81   have been found in various sites of the Mikulov area (Čtyroký, 1989; Čtyroký et al., 1990;

82   Březina, 2019). Therefore, studied sites in the Mikulov area must be always clearly specified.

83   Here we provide the first taxonomic review of the fossil vertebrates from the former

84   Czujan'sandpit. In addition, the combination of sedimentological, taphonomic and

85   taxonomical characteristics allows us to (1) determine the age of the site; and (2) provide a

86   reconstruction of the late Badenian terrestrial paleoenvironment of the northwestern part of

87   the Vienna Basin and adjacent southeastern part of the Carpathian Foredeep Basin, in areas

88   where the paleobotanical fossil record is rather poor.

89

90   **2. Czujan's sandpit and overview of research on Neogene vertebrates from the Mikulov**

91   **area**

92   The former Czujan's sandpit (also called Furstenälle, Fürstenwegfeld, Teichäcker or

93   Na Rybníkách) was a psephitic and psammitic quarry located 2 km east of Mikulov (Fig. 1A–

94   B; GPS: 48°47'49" N, 16°40'18" E) in the South Moravian Region, Czech Republic. The

95   mining activity began in the 1930s, reaching a maximum extension of 250 × 120 m and 7–10

96   m in depth. Exploitation of sands and gravels progressed from south to northwest and the

97   abandoned southern parts of the sandpit were gradually filled with garbage (Březina, 2019).

98   During the 1980s, Czujan's sandpit was filled to the top and leveled completely, being

99   currently part of a vineyard.

100   Czujan's sandpit stands out as the oldest Miocene vertebrate site of the Mikulov area,

101   which is located close the Carpathian Foredeep Basin. Indeed, vertebrate fossil remains have

102   been known from sandpits in the Mikulov area since the 19th century (e.g., Hörnes, 1848;

103   Alth, 1850). However, their contribution to a broader understanding of the European middle

104   Miocene paleoenvironments and faunas has been hampered by different conceptions about the

105   age of the various sites. Abel (1910) advocated an early Pliocene age, given the faunal

106   similarities with Eppelsheim (currently late Miocene, Pannonian), including the presence of

107   *Deinotherium giganteum*, *Chalicotherium* aff. *goldfussi*, *Hipparion gracile*, and *Chalicomys*

108   *jaegeri*. Stejskal (1934) agreed with the early Pliocene age suggested by Abel (1910), whereas

109   Rzehak (1922) dated it to the late Pliocene based on the absence of Pannonian mollusks

110   (*Congeria* and melanopsids). Jüttner (1938) first noted that the Mikulov area included several

111   Miocene vertebrate sites of different ages. In particular, Jüttner (1939a) interpreted Czujan's

112   sandpit as being Sarmatian in age, given petrographical similarities with the sands from

113   Chrastiny Hill, near Valtice, where Sarmatian mollusks are present. Such interpretation was

114   followed by many subsequent authors (e.g., Musil, 1956; Thenius, 1959; Seitl, 1985).

115   However, Buday et al. (1964) considered Czujan's sandpit as the highest strata of the late

116   Badenian (Kosovian substage) based on the foraminifers and mollusks. A Kosovian age was

117   later confirmed by comparison with nearby (800 m away) Nové Mlýny-2 borehole (Čtyroký,

118   1989; Fejfar, 1990; Čtyroký et al., 1990). Alternatively, some authors advocated that Czujan's

119   sandpit is "middle" Badenian (Wielician substage) in age, but such proposals were not

120   substantitated (Kuklová, 1978; Stráník et al., 1999; Jiříček, 2002), and changes in the

121   Badenian subdivision during time (see Kováč et al., 2018) make this assertion doubtful as

122   well.

123   A list of fossil mammals from Czujan's sandpit was first reported by Thenius (1951),

124   who erected the nominal species *Gazella stehlini* on the basis of a set of horn cores from

125   Czujan's sandpit (type locality) and Klein-hadersdorf (Austria), some of which are currently

126   housed at the Paleontological Institute of the University of Vienna (Weinfurter collection). In

127   addition, Thenius (1951) provided a faunal list from the site, including chelonians,

128   proboscideans, rhinocerotids, cervids, and chalicotheriids. Later on, Thenius (1979) erected

129   the genus *Caprotragoides* to accommodate ?*Pseudotragus potwaricus* (middle Miocene of

130   Fort Ternan, Kenya) as type species, as well as "*Gazella*" *stehlini* from Czujan's sandpit.

131   Subsequently, Azanza and Morales (1994) tentatively included *Caprotragoides stehlini* in

132   *Tethytragus* as ?*Tethytragus stehlini*. Some proboscidean molars from Czujan's sandpit have

133   also been described (Holec, 1985; Seitl, 1985) and ascribed to *Zygolophodon turicensis* and

134   *Gomphotherium angustidens*.

135

136   **3. Geological background**

137   Czujan's sandpit belongs to the Pannonian Basin System and is located on the

138   northwest margin of the Vienna Basin (Fig. 1A). In the Mikulov area, Neogene sedimentation

139   began by the deposition of marine lower Badenian clays (Lanžhot Beds) on the Mesozoic and

140   Paleogene flysch basement (Ždánice Unit). At that time, the Vienna Basin was connected with

141   the Carpathian Foredeep Basin by a narrow marine channel known as the "Mikulov Gate"

142   (Brzobohatý and Stráník, 2012). From a tectonic viewpoint, the Vienna Basin was

143   transformed into a pull-apart basin at the beginning of the "middle" Badenian (sensu

144   Harzhauser et al., 2018). The rivers flowed into the basin from the west through the Mikulov

145   area and apparently eroded the Lanžhot Beds (Stráník et al., 1999; Jiříček, 2002).

146   During the "middle" Badenian, the Sedlec Gravels were deposited discordantly on the

147   Ždánice Unit in the Mikulov area (Čtyroký et al., 1990). The overlying "middle" to "upper"

148   Badenian (sensu Harzhauser et al., 2018) marine deposits belong to the Hrušky Formation,

149   which has yielded a rich marine fauna (e.g., Kienberg locality; Brzobohatý et al., 2007). The

150   uppermost part of the Hrušky Formation terminates with alternating continental sands and

151   gravels, which contain the terrestrial vertebrate remains uncovered in Czujan's sandpit

152   (Čtyroký, 1989; Čtyroký et al., 1990).

153   In the Mikulov area, no Sarmatian deposits are known. The closest occurrences of

154   marine Sarmatian deposits are found at Chrastiny Hill near Valtice (Stráník et al., 1999).

155   Therefore, uppermost parts of the Hrušky Formation and even in the area of Mikulov were

156   eroded during the Sarmatian to the early Pannonian. Then, sands and silts (Bzenec Formation,

157   Pannonian; Fig. 1B) were deposited overlying the Badenian clays of the Vienna Basin and the

158   flysch basement (Ždánice Unit). Miocene sedimentation in the Vienna Basin terminates with

159   the uppermost Pannonian and Pontian sediments, mainly composed of gravels and cross-

160   bedded fluviatile sands (Valtice Beds; Čtyroký, 1989, 1999; Čtyroký et al., 1990). Generally,

161   Miocene sequences are covered by Quaternary deposits, such as fluvial and eolian sediments,

162   as well as paleosols (Čtyroký et al., 1990; Stráník et al., 1999).

163   The Czujan's sandpit deposits are constituted by fine- to coarse-grained sands

164   displaying a trough cross-stratification (Jüttner, 1939a). They are light gray to yellow in color

165   and mainly composed of quartz, quartzite, feldspar, and intercalated eolian quartz and diverse

166   pebbles (Patočková, 1966). Cerha (1987) noted that sands contain an admixture of gravels and

167   clays up to 50% (Fig. 3). According to Kuklová (1970), deposits overlying the Hrušky

168   Formation (i.e., Bzenec Formation and Valtice Beds, respectively, interpreted as Pannonian

169   and Pontian) have never been recorded from the borehole samples in the surroundings of

170   Czujan's sandpit (see also Čtyroký, 1989; Březina, 2019).

171

172   **4. Materials and methods**

173

174 4.1 Studied material

175   The fossil vertebrate material from Czujan's sandpit consists of 464 identified remains

176 collected between 1930 and 1970. They include teeth, skulls, postcranial bones, and turtle

177 shell remains (see complete list in the Supplementary Table 1). The studied material is

178 currently housed in the following institutions: PIUW, Paleontological Institut University

179 Vienna (Weinfurter collection), Austria; MZM, Moravian Museum, Brno, Czech Republic;

180 RMM, Regional Museum in Mikulov, Mikulov, Czech Republic; ÚGV, Department of

181 Geological Sciences, Faculty of Sciences, Masaryk University, Brno, Czech Republic. The

182 material housed in MZM includes the research collection of Rudolf Musil from the 1950s and

183 the remains gathered by private collectors between 1956–1959 (V. Solařík) and in 1965 (J.

184 Maňák). The material housed in MZM was prepared for this study by one of the autors (J.B).

185 However, a detailed description of the available material is beyond the scope of this paper,

186 which focuses instead on the most informative specimens from taxonomic, biostratigraphic,

187 and/or paleoecological viewpoints.

188

189 4.2 Sedimentology, taphonomy and biostratigraphy

190   Sedimentological and taphonomic analyses of Czujan's sandpit are restricted because

191 the site is no longer accessible and also field documentation is lacking. Sedimentological

192 interpretations were based on Jüttner's (1938, 1939a, 1940) lithological descriptions;

193 associated information preserved on labels; unpublished reports from the Czech Geological

194 Survey (Geofond, Prague); and old photos from the photoarchive of the Department of

195 Geology and Paleontology, MZM. As for the micropaleontological analysis, some samples of

196 clay and silt preserved in bone and tusk cavities were washed using a sieve with a mesh

197 diameter of 0.062 mm, and inspected using a stereomicroscope NIKON SMZ 1.

198   Given that fossil remains were recovered from the surface or the profiles of former

199   Czujan's sandpit without systematic excavation techniques or any documentation of their

200   provenance or spatial distribution, taphonomical analyses are restricted to the study of the

201   assemblage and bone modification data (see Eberth et al., 2007). A bias toward the collection

202   of the most complete fossils during fieldwork is unlikely, given the high number of rounded,

203   fragmentary and otherwise poorly preserved specimens available among the studied material

204   from MZM. The taphonomic analysis is focused on the degree of abrasion, corrosion, and

205   weathering of the bones. We mainly considered the completeness of the bones and their

206   degree of anatomical articulation with other elements to evaluate their preservation state. The

207   taphonomical terminology and practical approach follows Behrensmeyer (1991). We

208   quantified the minimum number of individuals (MNI) and the minimum number of elements

209   (MNE). Other aspects that were taken into account, include differences in tooth wear,

210   epiphyseal fusion, and morphology of fossil bones.

211   The European Neogene Land Mammal Units (Mein, 1975, 1990, 1999; de Bruijn et

212   al., 1992) do not display constustent boundaries throughout the Europe (e.g. Hilgen et al.,

213   2012; Koufos, 2016). Mammal zonation applied for the Central European area was modified

214   according to Steininger (1999), Becker (2003) and Hilgen et al. (2012). Age limits for well

215   dated Central European Miocene localities with their fossil record follows works listed in the

216   Supplementary Information.

217

218   **5. Results**

219   5.1 Sedimentology

220   The reconstruction of a composite profile was made using data obtained from the

221   individual boreholes in close proximity of the Czujan's sandpit (Fig. 2), which allow us to

222   define three facies associations (FAs; Fig. 3). The lower part of the composite profile (~80 m

223   thick) corresponds to FA1 (Wielician to Kosovian), constituted by clays with occasional sand

224   layers. FA2 (Kosovian) reaches a thickness of ~20 m and overlies FA1. Sporadic layers of

225   gravel appear at the base of the FA2, whereas its upper part consists of interbedded sand and

226   clay layers. The upper part of the profile corresponds to FA3 (Kosovian), which almost

227   reaches 20 m in thickness. It is characterized by the highest portion of coarse-grained deposits

228   (sands and gravels) over the clays. This facies association (FA1–FA3) represents a

229   coarsening-up sequence belonging to the Hrušky Formation. Czujan's sandpit was opened in

230   the uppermost part of the FA3, which contains the coarsest deposits. Both FA2+FA3

231   constitute a gravel-sand body up to ~600 m wide and ~45 m thick. This body is deposited

232   within clay-dominated deposits. Clayey sediments overlying FA3 (Fig. 3) and recovered in

233   the uppermost borehole S164 (Fig. 2) were not described and interpreted in detail due to the

234   cursory description of Cerha (1987).

235   The sedimentary architecture of the Hrušky Formation can only be studied in FA3

236   based on two historical photographs of the Czujan's sandpit profiles taken by R. Musil in

237   1964. The first profile shows co-sets of sand and gravelly sand with trough cross-stratification

238   (St, SGt; Fig. 4A) and co-sets of sand and gravelly sand with horizontal stratification (Sh,

239   SGh; Fig. 4A). Strongly eroded bases are recognized in the co-sets of facies (St, SGt) and the

240   individual sets (red and blue lines respectively; Fig. 4A). Some sections show the cross strata

241   onlap to the rising bases (white arrows; Fig. 4A). The individual sets (blue lines, Fig. 4A) and

242   the co-sets of facies Sh, SGh (green lines; Fig. 4A) have either subhorizontally or planar

243   bases. In contrast, the second profile (Fig. 4B) shows a sequence of two sedimentary units.

244   The lower unit is formed by co-set of planar cross-stratified sand (Sp facies), where individual

245   sets are separated by either planar or variously inclined surfaces (blue lines; Fig 4B). A large

246   body of clay (yellow arrow) is discerned in facies Sp (Fig 4B). This lenticular clay body was

247   originaly placed horizontally in the profile, but in fact it is partially deformed due to a partial

248   sliding of the sandpit wall (Fig 4B). In turn, the upper unit is formed by co-sets of sand and

249   gravel with low-angle cross stratification (co-sets of facies Sl, Gl; Fig 4B), where the bases of

250   the sets are faintly scoured (red lines; Fig 4B).

251

252   5.2 The faunal assemblage from Czujan's sandpit

253   The following sections report on the fossil vertebrates from Czujan's sandpit (see

254   updated faunal list with MNI in Table 1).

255

256   5.2.1 Reptiles

257   The herpetological assemblage only includes nine specimens of Testudines, of which

258   one belongs to a soft-shelled turtle and the remaining ones to a middle-sized testudinid.

259   PIUW-8X1939 (Fig. 5A) is a costal plate fragment, as shown by the presence of a rib on the

260   visceral part. Dorsally, the distinctive sculpturing consisting of small rounded pits, separated

261   from one another, allows us to refer the specimen to Trionychidae indet. (Marmi and Luján,

262   2012; Vitek and Joyce, 2015). Thenius (1951) reported from Czujan's sandpit the presence of

263   *Trionyx* sp. However, given that the sculpturing pattern does not allow distinguishing between

264   the two genera of soft-shelled turtles recorded from the Miocene of Central Europe (i.e.,

265   *Rafetus* and *Trionyx*; Georgalis and Joyce, 2017), identification at the genus rank is not

266   possible.

267   The remaining Testudines remains belong to a medium-sized testudinid, which was

268   reported as *Testudo* sp. by Thenius (1951). Four specimens have three-dimensionally

269   preserved carapace. The most complete shell (MZM Ot7877; Fig. 5B–C) is slightly elongated

270   and preserves the xiphiplastra (Fig. 5C), which indicates the lack of a hypo-xiphiplastral hinge

271   (Delfino et al., 2012). The peripherals 1–3 are not crossed by the pleuromarginal sulcus,

272   unlike in geoemydids (Luján et al., 2014). Peripherals 3–7 are completely involved in the

273 shell bridge and not elevated relative to overall shell height. Peripherals 8–10 are well

274 developed posteroventrally (Figs. 5B, 6G), but not curved medially as in *Testudo canetoniana*

275 (see Lapparent de Broin, 2000). The complete pygal shows that the supracaudal scute is not

276 divided by a sagittal groove. The anterior plastral lobe is trapezoidal and the anterior edge is

277 truncated (it does not protrude from the carapace contour). The neural 1 is subrectangular and

278 not constricted posteriorly. Based on these features, the *Testudo* specimens from Czujan's

279 sandpit are referred to *Testudo* (*Chersine*) *kalksburgensis*, which is only known from its type

280 locality (Wien-Kalksburg, Vienna Basin), dated to the Middle Miocene (MN5–MN6; Toula,

281 1896; Bachmayer and Młynarski, 1981; Luján, 2015; Luján et al., 2016, in press).

282

283 5.2.2 Mammals

284   Proboscidean remains belong to three genera from different families —

285 *Prodeinotherium* (Deinotheriidae), *Zygolophodon* (Mammutidae), and *Gomphotherium*

286 (Gomphotheriidae) — of which only the last one was mentioned by Thenius (1951).

287 Deinotheres are only represented by a single M3 (MZM Ot7526; Fig. 5D), which displays a

288 bilophodont occlusal pattern with a distally tapering contour, a moderately developed distal

289 cingulum, and a distinct convolute (postmetaloph ornamentation) close to the distal cingulum

290 at about crown midline. The small dimensions of this tooth (62 cm in length and 59 cm in

291 width) overlap with *Prodeinotherium* (Ginsburg and Chevrier, 2001; Gasamans et al., in

292 press) and enable to rule out the assignment to a species of *Deinotherium*. Although the two

293 European species of *Prodeinotherium* cannot be distinguished based on M3 morphology

294 (Ginsburg and Chevrier, 2001; Gasamans et al., in press), *Prodeinotherium cuvieri* is only

295 recorded from the early Miocene (Ginsburg and Chevrier, 2001; Böhme et al., 2012; Pickford

296 and Purabrishami, 2013; Gasamans et al., in press) so that a tentative assignment to

297 *Prodeinotherium* cf. *bavaricum* is warranted.

298   In turn, mammutid remains are the most abundant, being represented by dental as well

299   as cranial and postcranial remains. This is very exceptional for Mammutidae, which is much

300   less common than Deinotheriidae and Gomphotheriidae in the European Miocene (see

301   Göhlich, 2010). We concur with previous authors (Holec, 1985; Seitl, 1985) that

302   *Zygolophodon turicensis* is the only mammutid species recorded at Czujan's sandpit, as

303   supported by the morphological features displayed by the M3 (MZM Ot7519; Fig. 5E),

304   namely mesiodistally compressed lophs with well defined zygodont crests, long interlophs,

305   well-developed cingula, a disctinctly lower and narrower fourth loph, and a rhombic wear

306   pattern in the pretritte (Tobien, 1975, 1996; Tassy, 1977). Finally, only an M2 (MZM Ot7524;

307   Fig. 5F) and an upper tusk fragment (MZM Ot7505; Fig. 5G) testify to the presence of a

308   gomphothere. The M2 crown is trilophodont and displays a typical bunodont pattern (Tobien,

309   1973), with relatively thick enamel, an asymmetrical trefoil wear pattern in the pretritte, a

310   reduced lingual cingulum, massive cusps, and narrow interlophs that are blocked by enlarged

311   central conules. These characters allow us to discount the assignment of the material to the

312   early diverging species of the *Gomphotherium* (*annectens*) species group, and further

313   distinguish the Czujan's M2 from the subtapiroid dental pattern of the more derived species

314   *Gomphotherium subtapiroideum* and *Gomphotherium steinheimense* (see Gohlich, 2010;

315   Tassy, 2014). The tusk fragment has a pyriform cross section and is twisted, with a

316   helicoidally oriented enamel band. The latter morphology is characteristic of *G. angustidens*,

317   whereas the upper tusks of *G. subtapiroideum, G. steinheimense*, and *Archaeobelodon filholi*

318   lack torsion (Göhlich, 1998, 2010; Tassy, 2014). We therefore concur with Seitl (1985) that

319   the Czujan's gomphothere is attributable to *G. angustidens*.

320   Three perissodactyl families are represented at Czujan's sandpit: Chalicotheriidae,

321   Rhinocerotidae, and Equidae. Thenius (1951) already reported the presence of

322   *Chalicotherium grande* (currently in *Anisodon*; Anquetin et al., 2007), but the original

323   material has not been found. The currently available most complete material is represented by

324   a fourth metacarpal (MZM Ot7766; Fig. 5H). It displays a roundish distal facet and a deep

325   lateral ligament fossa, and the shaft is lateromedially compressed but widens distally. The

326   dorsal side of the shaft is straight, whereas the palmar side is concave. The concave palmar

327   side and the presence of a single facet for metacarpal III in the Czujan specimen distinguish it

328   from the morphology displayed by the schizotheriines, which display a more massive and

329   dorsoventrally compressed metacarpal IV with two separate facets for the metacarpal III

330   (Zapfe, 1979). MZM Ot7766 fits well in size and shape with the remains of *Anisodon grande*

331   from Devínská Nová Ves - Zapfe´s fissure (Zapfe, 1979) and Sansan (Guérin, 2012), whereas

332   *Chalicotherium goldfussi* shows slightly larger dimensions (Guérin, 2012).

333   Two rhinocerotid genera are recognized at Czujan's sandpit on the basis of different

334   limb bone proportions: *Hoploaceratherium* and *Brachypotherium*. The right complete tibia

335   MZM Ot7749 (Fig. 5I) displays more elongated proportions than in the teleoceratin

336   *Brachypotherium* (Fig. 5J) and compared with other long-legged rhinocerotid genera, it more

337   closely matches the morphology of *Hoploaceratherium* (Heissig, 2009, 2012). The shaft is

338   slenderer than in *Aceratherium* and the distal epiphysis is broader than in *Lartetotherium*

339   (Hünermann, 1989; Heissig, 2012). The caudal plane below the condyles is medially bounded

340   by a sharp ridge, and the frontal groove of tuberositas tibiae is narrow and centrally located.

341   These characters are typical for Aceratheriini and do not occur in *Lartetotherium* (Heissig,

342   2009, 2012).

343   In turn, the genus *Brachypotherium* is represented by dentognathic (an upper incisor

344   and a maxillary fragment) and postcranial (tibia) remains. The slightly worn I1 (MZM

345   Ot7700; Fig 5K) displays a short blunt root and differs from those of *Aceratherium* and

346   *Lartetotherium*, which are somewhat smaller and possess a pointed root (Heissig, 2012). In

347   turn, an assignment to *Hoploaceratherium* can be excluded due to the lack of upper incisors in

348   the latter genus (Heissig, 2012). The M2–M3 from the maxillary fragment MZM Ot7752 (Fig.

349   5L) display a brachyodont morphology, with a strong lingual cingulum surrounding the

350   protocone and extending to the base of the hypocone; the M2 has a weak buccal cingulum and

351   a well-developed crochet. These molars differ from those of Aceratheriini and Rhinocerotini

352   by their greater dimensions and stronger cingulum (Heissig, 2012). The complete left tibia

353   MZM Ot7752 (Fig. 5J) is relatively shorter and more robust than in the "long-legged"

354   Aceratheriini and Rhinocerotini (Cerdeño, 1993; Heissig, 2012), supporting an assignment to

355   *Brachypotherium*. The dimensions of M3 and tibia correspond well to those of

356   *Brachypotherium brachypus* from Malartic (MN7+8, France; Cerdeño, 1993), in agreement

357   with the previous report by Thenius (1951) of *B.* cf. *brachypus* from Czujan's sandpit based

358   on unknown material.

359   As for the equids, only an anchitheriine maxillary fragment with fragmentary M1 and

360   very worn M2 is available (MZM Ot7765; Fig. 5M). The molars are brachyodont and broader

361   than long; the metaloph and protoloph hooked in distal direction, and only a vestigial lingual

362   cingulum is present. Three anchitheriine species have been recorded from Central Europe:

363   *Anchitherium aurelianense*, *Anchitherium hippoides*, and *Anchitherium steinheimense*

364   (Abusch-Seiwert, 1983; Rotgers et al., 2011). However, we refer MZM Ot7765 to

365   *Anchitherium* sp. because the advanced degree of wear makes it impossible to ascertain

366   occlusal details.

367   Artiodactyls are represented at Czujan's sandpit by five taxa from four different

368   families: Bovidae, Palaeomerycidae, Cervidae and Suidae. The bovid material includes a

369   single frontoparietal with horn cores (MZM Ot7786; Fig. 5N–O). The horn cores are long,

370   straight, and moderately divergent, and display a mediolateral uniform compression and weak

371   longitudinal grooves from base to apex; the pedicels are tall (Fig. 5N–O). MZM Ot7786

372   represents the most complete material and fits well in size and shape with the material from

373 Czujan's sandpit and Klein-hadersdorf used by Thenius (1951) to erect "*Gazella*" *stehlini* and

374 subsequently assigned to ?*Tethytragus stehlini* by Azanza and Morales (1994; see also Bibi

375 and Güleç, 2008). We note that MZM Ot7786 is more complete than the holotype (only a

376 gypsum cast was inspected in PIUW) of *Te. stehlini*, which is represented by a single left horn

377 core fragment.

378 A palaeomerycid mandibular fragment with right m2–m3 is preserved (MZM Ot7773;

379 Fig. 5P). The lower molars display a rugose enamel surface (particularly on the lingual side)

380 and a brachyselenodont morphology with strong deep valleys and pointed conids (Fig. 5P).

381 This combination of features supports the attribution to Palaeomerycidae indet., but does not

382 enable a more refined assignment to a genus due to the absence of more complete cranial

383 material.

384 Three cervid antler fragments with consistent morphology are preserved. MZM Ot7771

385 (Fig. 5Q) is the most complete cranial appendage, where only the anterior branch and

386 proximal part of the pedicle are broken off. The antler is straight, laterally compressed and

387 bifurcated, without burr, but with extended, strongly sculptered base with longitudinal

388 grooves and ridges. The studied antlers clearly differ from coronate antlers of *Lagomeryx* and

389 *Paradicrocerus* (previously *Stehlinoceros*, see Böhme et al., 2012). MZM Ot7771 is

390 dichotomous and more closely resembles the antlers of *Heteroprox*, being distinguished from

391 other European genera by the absence of a burr (e.g., Heckeberg, 2017; Rössner et al., 2021).

392 The general morphology and dimensions of MZM Ot7771 only fit well with those of

393 *Heteroprox*, which is known by three species in Europe. The appendage allows an assignment

394 to *Heteroprox larteti* by the larger dimensions and stronger sculpture than those of *H. eggeri*

395 (see Rössner, 2010). Its smaller dimensions, more ellipsoid cross section of the pedicle and

396 short anterior prong, excludes an assignment to *Heteroprox moralesi* (see Rössner, 2010).

397 Suids are represented by two mandibular fragments that, based on their similar

398 preservation, might belong to the same individual (Fig. 5R): a right fragment with m1–m2

399 (RMM P11a) and a left one with a partial m3 preserving the distal crown portion (RMM

400 P11b). The moderately worn m1 (16.5 x 10.4 mm) and the less worn and larger m2 (19.0 x

401 12.7 mm) display a similar morphology, with thick enamel, a similarly narrow subrectangular

402 occlusal outline, conspicuous furrows between the main cusps and the central and distal

403 pillars, a well developed mesiobuccal cingulum, and a distinct hypoectoconulid. The distal m3

404 fragment displays a relatively short talonid that is only slightly tilted buccally, with the

405 hypoconulid surrounded by cingular cusplets. This morphology resembles the tetraconodont

406 genera *Conohyus* and *Retroporcus*, which have been the subject of taxonomic revision during

407 the last decade (Pickford and Laurent, 2014; Pickford, 2016) and are still a matter of debate

408 (van der Made, 2020). Pickford and Laurent (2014) designated a lectotype for *Conohyus*

409 *simorrensis* and provided an emended diagnosis of the species, distinguishing the genus

410 *Conohyus* from the new genus *Retroporcus* (see also Pickford, 2016), which includes material

411 previously assigned to *C. simorrensis* by various authors (e.g., van der Made, 1989; van der

412 Made and Salesa, 2004). Pickford and Laurent (2014) and Pickford (2016) interpreted

413 *Retroporcus matritensis* as a senior synonym of *C. simorrensis goeriachensis*, whereas van

414 der Made (2020) questioned the lectotype designation by Pickford and Laurent (2014) and

415 considered *R. matritensis* a junior synonym of *C. simorrensis*. The suid mandibular fragments

416 from Czujan's sandpit would be referrable to *C. simorrensis* sensu van der Made (2020), but

417 until Pickford and Laurent's (2014) lectotype designation is proven wrong, we prefer to

418 follow their concept of *C. simorrensis* and distinguish *R. matritensis* as a distinct species.

419 Although both species largely overlap in the size of their teeth, the proportions of the m1 and

420 m2 from Czujan's sandpit do not fit well with those of *C. simorrensis* sensu Pickford and

421 Laurent (2014), being relatively narrower and most closely resembling those of *R. matritensis*

422 (Pickford, 2013, 2016). The slightly tilted m3 talonid also more closely resembles the latter

species, since *C. simorrensis* is characterized by a less symmetrical talonid (Pickford and Laurent, 2014; Pickford, 2016). Although additional material (particularly the premolar series) would be required to confirm our identification, based on the aforementioned features we tentatively assign the material to cf. *R. matritensis*. Similarly to *C. simorrensis*, *R. matritensis* is known from European localities ranging from MN5 to MN9 (Pickford and Laurent, 2014; Pickford, 2016).

The carnivoran remains from Czujan's sandpit consist only of two partial lower canines (ÚGV Pal297, Fig. 5S; MZM Ot7814) and a calcaneum (MZM Ot7815; Fig. 5T). The more complete canine (>8.2 cm in height) preserves the entire root and most of the crown (except for the apex; ÚGV Pal297; Fig. 5S). The base of the crown is labiolingually compressed and preserves a distinct wide lingual wear facet to accommodate the I3 (Fig. 5S). In mesiodistal view, ÚGV Pal297 is slightly sigmoidal, which is typical for several groups of carnivorans. According to Viranta (1996), two valid amphicyonid genera are known from the middle Miocene of Europe: *Megamphicyon giganteus* (MN3–MN5), until recently included in *Amphicyon* (Siliceo et al., 2020); and *Amphicyon major* (MN4–MN9). The canine root of ÚGV Pal297 is less robust than in *Megamphicyon giganteus* (see Kuss, 1965). Based on size and root proportions, both canines are thus referred to *Amphicyon* (Ginsburg, 1961; Ginsburg and Antunes, 1968). The calcaneum MZM Ot7815 (Fig. 5S) is slightly abraded, especially the tuber calcanei, but it preserves enough diagnostic features to further support the assignment to *Amphicyon*. It is relatively short (8 cm long) and displays a robust tuber calcanei. The ectal facet is convex, craniocaudally elongated, and completely separated from the sustentacular facet. The latter is rather flat, semicircular in outline, and medially protruding. The referral to *Amphicyon* is based on size as well as the robustness of the tuber calcanei and the shape of the ectal facet (Argot, 2010). Given the restricted available material, we only tentatively assign the material to *Am.* cf. *major*.

448

449   5.3 Taphonomy

450   Despite the lack of field documentation, many fragmentary remains could be joined

451   into complete bones during material preparation. This fact, and the presence of fresh fractures

452   on the bone fragments, indicate that they were well-preserved and generally complete in the

453   field, but that they were not adequately collected due to the "rescue" character of the

454   excavations. Bones and teeth without any sign of transportation include 91% of the studied

455   material, and 31% of the studied material represents complete skeletal elements from various

456   parts of skeletons: teeth, skull fragments, mandibles, vertebrae, ribs, scapula, humerus, ulna,

457   radius, and autopodial bones. The preservation of the vertebrate remains from Czujan's

458   sandpit may be summarized as follows: 1) there is a high number of complete bones and teeth,

459   being the former more frequent than the latter; 2) teeth are preserved both as dentognathic

460   fragments (Fig. 5G, L, M, P, R) and isolated tooth crowns with roots (e.g., Fig. 5D, E, F, K,

461   S); 3) we identified up to 29 cases of antimere bones (e.g., right and left humerus: Fig. 6A–B)

462   and teeth; 4) in 10 cases, different bones appear to belong to the same individual and have

463   been preserved in articulation or close spatial association, based on anatomical congruence,

464   preservation state and/or information from labels (Fig. 6C–E), while in four cases unfused

465   epiphyses matched with the corresponding diaphysis (Fig. 6F); 5) as pointed out by Jüttner

466   (1938), there were well-preserved proboscidean skulls in Czujan's sand pit (either not

467   recovered or subsequently disintegrated); 6) four of the seven testudinid specimens preserved

468   well their 3D morphology and growth scute lines are discernible in some carapace plates

469   (Figs. 5B, 6G). The presence of antimeres and articulated specimens among the proboscidean

470   sample, coupled with similar preservation, indicates that most of the bones come from a

471   single individual—as further supported by information from the museum label of the

472   proboscidean atlas RMM P34, according to which it was articulated with the skull in situ.

473   Generally, all bones and teeth are strongly mineralized in a similar way (Březina,

474   2019), and the mineralization of the more rounded and abraded bones is comparable with

475   most of the better preserved ones, suggesting the lack of reworking and resedimentation of

476   fossils from older deposits. Bone cavities are filled by quartzose sands, gravels, and clays.

477   Finally, some specimens (e.g., MZM Ot7497 and MZM Ot7694) may contain remnants of soil

478   or plant roots. Most of the fossil bones are fresh and angular (Figs. 5B–C, G, H–J, N–O; 6A–

479   D, G-H) and only rarely are deformed (Fig. 6I). Prediagenetic traces of bone corrosion are

480   infrequent. Only weathering stage 1 (sensu Behrensmeyer, 1978) modifications were

481   observed, although longitudinal cracks in diaphyses and articular facets are often present (Fig.

482   6I–J). Two gnawing traces, probably produced by some large carnivores (Fig. 6K–L) and a

483   rodent, were identified (Fig. 6M). However, we cannot exclude that some gnawing traces

484   were alternatively produced by a ruminant, as they show a similar pattern to those produced

485   by rodents (Hutson et al., 2013).

486   Most of the studied material belongs to terrestrial vertebrates and shows no signs of

487   redeposition. In contrast, rare marine fossils indicate redeposition (Seitl 1985). In particular,

488   the analyzed pelitic matrix taken from the fossil bones only sporadically contains microfaunal

489   marine remains, including: a single placoid shark scale; and the following foraminifera

490   (*Arenobulimina* sp., *Amonodiscus* cf. *glabratus*, *Paragloborotalia acrostoma*, *Heteroleppa*

491   *dutemplei*, and Globigerinida indet.), which must have been redeposited from the lower

492   Badenian Ždánice Unit (R. Brzobohatý and M. Bubík, pers. comm. to J.B.) as well as a single

493   isolated shark tooth crown (Fig. 6N) referred to *Isurus* sp. The macroflora is represented by

494   non-redeposited scarce wood remains (Fig. 6O), whereas palynomorphs were not present in

495   the analyzed sediment samples.

496   All recovered testudinids from Czujan's sandpit are adult individuals, not only based

497   on size, but further because the sutures between plates are completely fused or poorly visible

498   in some cases. Based on the third molar eruption and/or epiphyseal fusion, mammals from

499   Czujan's sandpit are adult individuals, with the only exception of proboscideans. Ontogenetic

500   analysis, based on dental wear stages in the proboscidean samples (see Tassy, 1996, 2013),

501   revealed different ontogenetic stages, including three juveniles, two mature subadults and

502   fifteen midlife adults (Table. 2).

503

504   **6. Discussion**

505   6.1 Sedimentological interpretation

506   From a sedimentological viewpoint (Figs. 3–4), the original outcrops of Czujan's

507   sandpit were formed by tabular bars (Sh, SGh) and channel infills (St, SGt, Sp), which fill the

508   distributary channels of both deltaic plain and deltaic front of a shallow water fluvial

509   dominated delta (Postma, 1990; Chen et al., 2015; Zhang et al., 2017). The onlaps of cross

510   strata arise during migration of climbing dunes in mouth bars of a delta front (Dasgupta et al.,

511   2016), whereas the superposition of co-set facies Sl, Gl over co-set facies Sp can be

512   interpreted as delta plain deposits overlapping mouth bar sediments (Francírek, 2018). The

513   clay body (Fig. 4B) is most probably interdistributary bay infill (Zhu et al., 2017). As is

514   typical for braid deltas, the delta plain is composed only by distributary channel infills

515   (McPherson et al., 1988). Both the coarsening-upward sequence of facies association FA1–

516   FA3 and the lens shape of megascale body FA2+FA3 reflect a delta progradation into a

517   marine basin. According to this interpretation, three facies associations are recognized: FA1,

518   composed by pelagic sediments; FA2, prodelta sediments (suspension clays plus occasional

519   sand turbidites) up to the delta slope sediments (sand turbidites plus suspension sediments of

520   quiet phase on delta slope); FA3, sediments of delta front (mounth bars and interdistributary

521   bays) and delta plain (subaerial distributary channels) infills. The latter interpretation is

522   supported by the occurrence of wood fragments (Fig. 6O), which are common in distributary

523   channels or their mouth along the delta front (Olariu and Bhattacharya, 2006), as well as by

524   the presence of terrestrial fauna. Based on the sedimentary architecture, Czujan's sandpit can

525   be interpreted as a shallow-water river delta with braid delta plain and with mouth bars in

526   distributory outlets and interdistributary bays on delta front (Nemec, 1990; Postma, 1990; Zhu

527   et al., 2017).

528

529   6.2 Taphonomical interpretation

530   The bone concentration from Czujan's sandpit is characterized by the relatively diverse

531   assemblage of terrestrial vertebrates, the presence of complete and associated bones (skull

532   bones, mandibles, vertebrae, ribs, limb bones), a low degree of weathering, and a

533   predominance of fresh and angular specimens. These aspects, and the absence of polished or

534   otherwise discrepant bone of terrestrial vertebrates characteristic for exhumation or

535   redepositions (Rogers and Kidwell, 2007), unequivocally indicates that the terrestrial

536   vertebrate assemblage is not mixed with reworked older terrestrial fossils. In contrast, the rare

537   marine fossils represent redepositions from the Ždánice Unit, Lanžhot Formation and lower

538   parts of Hrušky Formation (Seitl 1985). Reworked, allochthonous marine fossils have been

539   already documented by Kuklová (1970, 1978) from the Wielician-Kosovian clays in

540   boreholes (Figs. 2, 3).

541   The presence of bones and teeth from more than a single individual and with multiple

542   species represented allows us to classify at least the sands and gravels of FA3 (vertebrate

543   remains are not documented from sands and gravels of FA1–FA2) as a macrofossil multitaxic

544   bonebed (Behrensmeyer, 2007; Eberth et al., 2007; Rogers and Kidwell, 2007). Because

545   mining extraction in Czujan's sandpit from the 1930s to the 1980s progressed from south

546   towards north and east, and abandoned parts of the sandpit were gradually filled by waste as

547   extraction progressed, new and relatively small outcrops (in comparition with the whole

548   mining area) were accessible in each mining phase (Březina, 2019). This implies that more

549   than a one bone bed was present in the Czujan's sandpit profiles. The different types of rocks

550   represented by the matrix adhered to the fossils as well as the presence of recent soil remnants

551   on some specimens suggest that the fossil remains came from different stratigraphic positions.

552   This is further supported by the old label of PIUW 4501–4503, which clearly describes the

553   find at 6.5 m depth, and corresponds well with Seitl's (1985) observation that bones and teeth

554   were vertically scattered along the whole profile. Therefore, from a finer scale perspective, we

555   can conclude that the bone accumulations of FA3 were located in more than one chanel infill,

556   probably as a result of gradual or periodical fluvial sedimentation. In the absence of field

557   documentation, it is impossible to confidently establish whether the fossil bones originated

558   from a time-averaged accumulation of carcasses randomly transported from the river basin

559   and deposited due to the loss of water energy along the mouth of distributary channels into the

560   sea. Alternatively, the assemblage might have originated by the progressive accumulation

561   from a preexisting source of mass death accumulation. However, the high concentration of

562   terrestrial taxa is outstanding in the context of surrounding marine deposits, and the low

563   number of carnivorans and the presence of a single specimen of a freshwater taxon

564   (trionychid) rule out either a flooding event or a miring mortality (Rogers and Kidwell, 2007).

565   Moreover, multitaxic fossil assemblages, formed by immature individuals as well as gnawing

566   traces, do not occur in mass drowning (Rogers and Kidwell, 2007; Backwell et al., 2018).

567   Both the presence of cracks and the gnawing traces suggest that some carcasses were laying

568   for some time on the surface before sediment deposition.

569   The main taphonomic features of the Czujan's sandpit assemblage (i.e., wearing stage

570   1 sensu Behrensmeyer, 1978, a minimal number of gnawed bones, and evidence for

571   articulated skeletons) are often reported from drought mass death sites (Haynes, 1985, 1988,

572   1991, 2018, Backwell et al., 2018). The structure and MNI of taxa such as proboscideans,

573   bovids or testudines from Czujan's sandpit (Table 1) further resemble those from extant sites

574   from Africa, where drought mass death implies a higher mortality of proboscideans and

575   bovids (Haynes, 1988). Predominance of large herbivores such as proboscideans (Table 1),

576   which are characterized by high mortality during dry periods, might support this idea

577   (Haynes, 1985, 1991, 2017; Haynes and Klimowicz, 2015). Variously old proboscidean

578   individuals have been recovered from Czujan's sandpit fossil record, including juveniles

579   (Table 2), which are characteristic in recent drought mass death sites (Haynes, 1985, 1991,

580   2017; Haynes and Klimowicz, 2015). Based on our findings, a progressive secondary

581   accumulation from preexisting drought mass death accumulations into FA3 seems most

582   likely. This interpretation would be in agreement with the strong decrease of humidity in

583   Central Europe during the late Badenian, as well as the presence of seasonality in the Vienna

584   Basin accompanied by periodic drought conditions (e.g., Böhme et al., 2011; Harzhauser et

585   al., 2011), supported by documented braid delta. This delta type occurs in areas with arid

586   climate and limited vegetation, fed by flows with unbalanced flow rate (McPherson et al.,

587   1988; Miall, 1996). However, poor field data do not allow to clearly determine if the fossil

588   assemblage is a time-averaged abiotic accumulation or whether it was deposited following

589   drought mass death accumulation. Taking in account the dispersal capabilities of large

590   mammals, the studied taphocoenosis probably mixes taxa from various biotopes concentrated

591   in one place of the river basin for both possible intepretations. In the analogy with recent

592   elephant populations whose home ranges reach up to ~3000 km^2 (Haynes, 1991), we assume

593   that animals might have inhabited area from the Vienna Basin coastline, including delta

594   platform to the eastern slopes of Bohemian Masiff, which is largely formed by the

595   soutwestern part of the Carpathian Foredeep Basin (see Fig. 1).

596

597   6.3 Biostratigraphy

598   All mammal taxa identified in the Czujan's sandpit have been reported from the

599   European early Astaracian (MN6) localities. Although the mammal community as a whole

600   displays a wide biostratigraphic range from MN3 up to MN10, the first occurrence of *R.*

601   *matritensis* and *Hoploaceratherium* in Göriach, Austria (late MN5, ~14.5 Ma; Aiglstorfer et

602   al., 2014), and *Te. stehlini* in Klein-hadersdorf, Austria (MN5-MN6, ~14.2 Ma; sensu Böhme

603   et al., 2012) together with the last known occurrence of *P. bavaricum* from Devínska Nová

604   Ves-Zapfe's fissures, Slovakia (early MN6; Fejfar 1990) restrict the biostratigraphic age of

605   the Czujan's sandpit assemblage within the late MN5 to late MN6 Zones (Fig. 7). Given by

606   the fossil record of mammals from well-dated Central European localities, the above

607   mentioned biostratigraphic age is supported by the coeval first appearance of *R. matritensis*

608   and *Te. stehlini* and the last appearance of *P. bavaricum*, *Retroporcus matritensis*, *H. larteti*

609   and *Am. major* (Fig. 7). The Badenian age of the vertebrate assemblage is also partially

610   supported by the presence of a testudinid *T. kalksburgensis* reported from Wien-Kalksburg,

611   Austria (MN5–MN6; Bachmayer and Młynarski, 1981).

612   The biostratigraphical age (late MN5, to late MN6; late early to late Badenian; Fig. 7),

613   based exclusively on the vertebrate assemblage, is generally in agreement with the late

614   Badenian age of the Czujan's sandpit, as previously suggested based on marine and brackish

615   microfauna (Kosovian: Buday et al., 1964; Čtyroký, 1989; Čtyroký et al., 1990; Fejfar, 1990

616   and Wielician: Kuklová, 1978; Stráník et al., 1999; Jiříček, 2002). These authors did not

617   verify the age on the basis of vertebrate fauna, such as Thenius (1951) and Musil (1956) and

618   Seitl (1985), who adopted Jüttner's (1938, 1940) exclusively petrographic correlation with the

619   Sarmatian sands. However, Sarmatian age is highly improbable, because Sarmatian sediments

620   have not been documented from the Mikulov area (Fig. 1B). The presence of the *Ammonia*

621   *beccarii* ecozone, laterally replaced by the *Bulimina-Bolivina* Zone in the Nové Mlýny-2

622   borehole (Bimka, 1983), proves that both FA3 and FA2, together with the uppermost section

623   of FA1, correspond to the Kosovian substage (Figs. 2–3). The lower limit of the Kosovian

624   substage varies within the range of 13.6–13.1 Ma (Hohenegger et al., 2014) and therefore,

625   Czujan's sandpit assemblage cannot be older than ~13.6 Ma. This corresponds to the upper

626   MN6 boundary in Central Europe (base of C5ABn sensu Steininger, 1999, but see different

627   MN Zonation in Western Europe, Fig. 7).

628   According to the Nové Mlýny 2 borehole (Bimka, 1983), the section of Kosovian

629   continues minimally for at least ~40 m above the sandpit, however, the original thickness of

630   Kosovian section was most probably greater but subsequently reduced by Sarmatian and

631   Quarternary erosions. Therefore, both the close proximity to the Wielician/Kosovian

632   boundary (Fig. 2, 3) and mammal biochronology (Fig. 7) support latest MN6 (~13.6 Ma) age

633   of the Czujan's sandpit. *Prodeinotherium* and possibly also *Am. major* from Czujan's sandpit

634   are among the youngest records of these taxa from Central Europe (late MN6, Kosovian

635   substage; Fig. 7).

636

637   6.4 Paleoecological implications

638   The vertebrate assemblage from Czujan's sandpit comes from various paleohabitats. A

639   closed woodland habitat is indicated by proboscideans (*Prodeinotherium* cf. *bavaricum* and

640   *Zygolophodon turicensis*), rhinos (*Brachypotherium brachypus* and *Holoaceratherium* sp.),

641   chalicotheres (*Anisodon grande*), palaeomerycids, suids (*Retroporcus matritensis*) and

642   carnivorans (*Amphicyon* cf. *major*; Fig. 8). The dental morphology and the still rather limited

643   number of δ^{13}C values from tooth enamel of *P. bavaricum* (Seegraben; Aiglstorfer et al.,

644   2014) and *B. brachypus* (Steinheim; Tütken et al., 2006) indicate that both species might have

645   inhabited a closed woodland environment. Mammutids of the genus *Zygolophodon* browsed

646   in forest habitats as well (e.g., Lambert and Shoshani, 1998) but based on zygolophodont

647   deintition their dietary spectrum was most probably different from that of bunodont

648 gomphotheres and lophodont deinotheres. This assumption is indirectly supported by feeding

649 preferences of conifers (*Taxodium*) in closely related American mastodons (*Mammut*

650 *americanum*) from the Pleistocene of Florida (Green et al., 2005), where *Taxodium* swamps

651 are comparable to those documented from the Miocene of Central Europe (e.g., Kvaček et al.,

652 2004; Kázmér, 2007). The brachyodont teeth of palaeomerycids, as well as their isotopic data

653 from middle Miocene localities of Germany and Spain, support a folivorous diet in woodlands

654 (Tütken et al., 2006; Tütken and Vennemann, 2009; Domingo et al., 2012). A woodland

655 habitat is also favored by the chalicotheriid *A. grande*, which is considered a specialized

656 browser (Schulz et al., 2007), as well as the amphicyonid *Am. major*, which was an active

657 omnivorous predator (Argot, 2010) anatomically well-adapted for climbing trees and chasing

658 preys (Argot, 2010).

659   The presence of mixed-feeders such as *Gomphotherium, Anchitherium, Heteroprox*

660 and *Tethytragus* suggest, in addition, the existence of more open environments. The genus

661 *Gomphotherium* has been considered an inhabitant of open environments similar to recent

662 African savannas (Tassy, 1977; Lambert, 1996; Lambert and Shoshani, 1998). The isotopic

663 data for subtapiroid species of *Gomphotherium* from the latest early and early middle

664 Miocene of Germany suggests the consumption of C3 vegetation in woodland environments,

665 as documented by δ^{13}C values in *G. steinheimense* (−10.7‰ up to −10.1‰; Tütken et al.,

666 2006) and *G. subtapiroideum* (−11.9‰ to −10.2‰; Tütken and Vennemanm, 2009). However,

667 dental microwear studies of both species indicate a mixed-feeding, with *G. subtapiroideum*

668 likely favoring more open woodlands (Calandra et al., 2008, 2010). In contrast, the rather high

669 δ^{13}C values for *G. angustidens* from the middle Miocene localities of the Madrid Basin, Spain

670 (−10.65‰ to −6.21‰; Domingo et al., 2009, 2012) indicate that *Gomphotherium* might have

671 intruded into open and grassland environments. Although data from the Central European

672 populations of *G. angustidens* are missing, this species most probably favored more open

673 environments than the other proboscidean species recorded from Czujan's sandpit (i.e., *P.*

674 *bavaricum* and *Z. turicensis*), which most probably occupied a different ecological niche in

675 more closed woodland (Fig. 8). *Anchitherium* might also have inhabited open woodland

676 environments, as suggested by results from dental mesowear (Kaiser, 2009) and isotopic

677 studies (Tütken et al., 2006; Tütken and Vennemann, 2009) of *A. aurelianense* populations

678 from Sandelzhausen and Steinheim (Germany), as well as more open environments as

679 suggested by δ^{13}C values (–12.7‰ to –6.49‰; Domingo et al., 2012) from populations of

680 Spanish MN5–MN6 localities.

681   Mixed-feeding *Heteroprox* species usually inhabited forests or woodlands in Central

682 Europe (specifically Seegraben, Austria and Sandelzhausen, Germany) during the Langhian,

683 as documented by δ^{13}C values (–12.0‰ to 10.4‰; Tütken and Vennemann, 2009; Aiglstorfer

684 et al., 2014). However, the dental microwear study of *H. larteti* populations from central

685 Spain (DeMiguel et al., 2011), contrary to isotopic studies of Domingo et al. (2012), revealed

686 a high degree of grazing interpreted as an adaptation to seasonal arid periods during the

687 Serravallian. A similar variation in paleohabitat is recorded in *Tethytragus*. Isotope data of

688 *Tethytragus* sp. from Gratkorn, Austria (MN7+8; Aiglstorfer et al., 2014) indicate a woodland

689 environment, whereas isotope data of *Tethytragus langai* from Paracuellos 3, Spain (MN6;

690 Domingo et al., 2012) show a mixed-feeding diet related to more open conditions. Augustí

691 and Antón (2002) pointed out that *Tethytragus* was capable of inhabiting different habitats

692 with a diet comprising a variety of vegetation. This was confirmed by micro- and mesowear

693 analysis of *Tethytragus langai* from the Serravallian of Spain (DeMiguel et al., 2011). Hence,

694 seasonal variations of dietary composition in Central European populations (e.g., those from

695 Gratkorn) could have occurred as well (Aiglstorfer et al., 2014). The omnivorous *Retroporcus*

696 *matritensis* also preferred a more open woodland environment based on isotopic studies

697 (Tütken et al., 2006; Domingo et al., 2009).

698   Among rhinocerotids, *Brachypotherium brachypus* has been traditionally considered a

699   semiaquatic species of open environments (Heissig, 1999; Augustí and Antón, 2002; Costeur

700   et al., 2012). However, its brachyodont dentition, and the isotopical data of *Brachypotherium*

701   from Steinheim (MN7, Germany) and Eichkogel (MN11, Austria), suggest browsing in closed

702   woodland environment (Tütken et al., 2006; Aiglstorfer et al., 2014) unlike

703   *Hoploaceratherium*, which most likely favored more open environments based on δ^{13}C values

704   from the middle Miocene (MN5–MN6) localities from the Madrid Basin, Spain (–11.15‰ to

705   –9.02‰; Domingo et al., 2012). The different paleoecological preferences of these two

706   rhinocerotids are as well manifested with their anatomical differences, as *Hoploaceratherium*

707   has long legs and is better adapted for a cursorial locomotion in an open landscape, whereas

708   *B. brachypus* is a short-limbed and hippo-like species (Cerdeño, 1993; Heissig, 2012).

709   The indeterminate trionychid turtle is indicative of the presence of permanent

710   freshwater reservoirs, whereas the testudinid *Testudo kalksburgensis* inhabited open

711   woodland, or even more open environments. Medium-sized testudinids are well adapted to

712   dry conditons, and can inhabit a wide variety of open environments ranging from clearings

713   with low vegetation to semiarid habitats (Miklas-Tempfer, 2003, 2005; Čerňanský et al.,

714   2012; Luján et al., in press). The aquatic trionychid turtle, semiaquatic *Brachypotherium*

715   together with the rich fossil record of proboscideans at Czujan's sandpit, (whose recent

716   representatives are well known for water seeking; e.g., Haynes, 1991), further indicates the

717   presence of permanent freshwater bodies occurring in the northwest area of the Vienna Basin

718   coastline to the adjacent Carpathian Foredeep Basin. Middle Miocene changes in the Central

719   Paratethyan terrestrial environments were conditioned by increased tectonic activity which

720   resulted in uplifting mountains in the east and two marine transgressions, one during the early

721   Badenian and second one in the late Badenian (Kováč et al., 2007). The extensive areas

722   around the Vienna Basin were divided by the uplift of its eastern part into western lowlands

723 and eastern steep highlands in the late Badenian (e.g., Kvaček et al., 2006; Kováč et al.,

724 2007). The late Badenian paleobotanical record from eastern Central Europe indicate that the

725 highland situated southeast of the Vienna Basin was covered by a mixed mesophytic forest

726 with extrazonal (mountain) vegetation (i.e., Devínska Nová Ves, Slovakia; Kvaček et al.,

727 2006; Kováčová et al., 2011; Kovar-Eder and Teodoridis, 2018). The dominance of forest

728 environments is also documented in this area by the late Badenian mammal assemblages from

729 Devínska Nová Ves locality - Zapfe's Fissures, "Bonanza" and Sandberg (Sabol and Kováč,

730 2006). Although paleobotanical record from lowlands situated in the Carpathian Foredeep

731 Basin, (i.e., northwest of the Vienna Basin) is rather incomplete, recent analyses from the

732 early late Badenian to early Sarmatian low altitude (0-300 m a.s.l.) localities of the Carpathian

733 Foredeep Basin, together with the data obtained both south and west of the Vienna Basin,

734 point to the presence of subhumid sclerophyllous vegetation (Kovar-Eder and Theodoridis,

735 2018). The paleoecological analysis of the late Badenian Czujan's sandpit revealed a mosaic

736 of habitats represented by forests, close to open woodlands, more open environments, and

737 stagnant or slowly flowing freshwater reservoirs in the continental northwestern area of the

738 Vienna Basin to the adjacent Carpathian Foredeep Basin (Fig. 8). This mosaic of local

739 habitats could be understood as restricted riparian and floodplain forests surrounded by

740 widespread woodland which opened inland, locally passed into the more open environments

741 (grass dominated).

742 Subhumid sclerophyllous forests documented from the Central Paratethys suggest a

743 more marked precipitation seasonality for the late Langhian to early Serravalian period

744 (Kovar-Eder and Theodoridis, 2018). The predominance of open habitats, both west of the

745 Vienna Basin and in the southwestern part of the Carpatian Foredeep Basin (see also section

746 5.3.; table 1 and 2) is in agreement with increase in precipitation seasonality reported since the

747 early Badenian. This climatic change was mainly result of tectonically inferred sea-level falls

748 in West Carpathian-North Pannonian Basins (Kováč et al., 2001), as well as a possible

749 decrease of moist air mass production during the early Badenian (Böhme, 2003). The second

750 period of increased precipitation seasonality 14.7–14.5 Ma (Böhme, 2003), which most

751 probably persisted in the northwestern part of the Vienna Basin up to the early/late Badenian

752 transition, was followed by a late Badenian steep decrease of humidity in Central and Eastern

753 Europe. This drop in humidity culminated during the latest Badenian and Sarmatian stages

754 (~13–12 Ma; Böhme et al., 2008) as also documented by the dramatic succession of dry years

755 with irregular precipitation events recorded from isotopic record of Serravallian oyster shells

756 from the Vienna and Korneuburg Basins (Harzhauser et al., 2011).

757

758 **7. Conclusions**

759 Here we provide an updated faunal list of the middle Miocene vertebrate assemblage from

760 Czujan's sandpit site as well as interpretation of the geological, taphonomical and

761 paleoenvironmental data based on the osteological and dentognathic materials. A total of 14

762 vertebrate taxa were indentified, including two reptiles (**Testudines:** Trionychidae indet. and

763 *Testudo kalksburgensis*) and 12 mammals (**Proboscidea:** *Prodeinotherim* cf. *bavaricum*,

764 *Zygolophodon turicensis*, *Gomphotherium angustidens*; **Rhinocerotidae:** *Hoploaceratherium*

765 sp., *Brachypotherium brachypus*; **Chalicotheriidae:** *Anisodon grande*, **Equidae:**

766 *Anchitherium* sp.; **Suidae:** cf. *Retroporcus matritensis*; Palaeomerycidae indet.; **Cervidae:**

767 *Heteroprox larteti*; **Bovidae:** *Tethytragus stehlini* and **Carnivora:** *Amphicyon* cf. *major*). The

768 taphonomic analysis indicates that terrestrial vertebrate fossils could not be redeposited.

769 Fossil vertebrates from Czujan's sandpit come from deposits of a braid delta plain to delta

770 front deposited during the Kosovian substage (late Badenian). Based on the combination of

771 biostratigraphic and geological data, we assume that Czujan's sandpit age can be placed to

772 latest MN6 for Central Europe (close to Wielician/Kosovain substage boundary: ~13.6 Ma).

773 We conclude that there are two plausible explanations for the genesis of the fossil

774 accumulation from Czujan's sandpit, including: 1) an abiotic time-averaged concentration

775 generated by the transport energy of water; or 2) the gradual or periodical transport of remains

776 from one or more (in the case of more time-averaged as well) mass death site accumulation.

777 However, under both interpretations, the Czujan's sandpit vertebrate assemblage would

778 reflect an averaged spectrum of species from the whole river basin flowing into northwest of

779 the Vienna Basin. We suggest a mosaic of continental habitats in the area from northwestern

780 coast of the Vienna Basin to the adjacent Carpathian Foredeep Basin. These habitats were

781 represented by the restricted riparian and floodplain forests, surrounded by the widespread

782 woodlands opening locally into more open environment, with enough freshwater sources that

783 could eventually evaporate on a seasonal basis during droughts, leading to mass deaths of

784 animals.

785

786 **Authors Contributions**

787 J.B. and M.I. conceived and designed the study. J.B. prepared and catalogued the material

788 from MZM, compiled and analysed data from all studied specimens, and prepared the initial

789 manuscript draft (geology, taphonomy, paleoecology, biostratigraphy). J.B, M.I and À.H.L

790 prepared figures and tables. D.M.A., M.I., M.H., and À.H.L. analyzed data and wrote

791 additional sections of the manuscript (M.H.: sedimentology; D.M.A: Suidae and

792 Deinotheriidae; À.H.L.: Testudines and Carnivora). All authors improved the initial

793 manuscript draft equally and approved its final form.

794

795 **Acknowledgments**

796

815

References

817 Abel, O., 1910. Erläuterungen zur geologischen Karte der österreichisch-ungarischen

818   Monarchie, NW, Gr., Nr. 85, Zone 10, Koll. XV, Blatt Auspitz und Nikolsburg. Verl. K.-

819   K. Geol. Reichsanst. Wien, 1–37.

820   Abusch-Siewert, S., 1983. Gebissmorphologische Untersuchungen an eurasiatischen

821   Anchitherien (Equidae, Mammalia) unter besonderer Berücksichtigung der Fundstelle

822   Sandelzhausen. Cour. Forsch. Senckenberg 62, 1–401.

823   Aiglstorfer, M., Bocherens, H., Böhme, M., 2014. Large mammal ecology in the late Middle

824   Miocene locality Gratkorn (Austria). Paleodivers. Paleoenviron. 94, 189–213.

825   https://doi.org/10.1007/s12549-013-0145-5

826   Alth, A., 1850. *Dinotherium giganteum* von Nikolsburg. Ber. Mitt. Freunden Naturw. Wien 4,

827   7.

828   Anquetin, J., Antoine, P.-O., Tassy, P., 2007. Middle Miocene Chalicotheriinae (Mammalia,

829   Perissodactyla) from France, with a discussion on chalicotheriine phylogeny. Zool. J. Linn.

830   Soc. 151, 577–508. https://doi.org/10.1111/j.1096-3642.2007.00327.x

831   Argot, C., 2010. Morphofunctional analysis of the postcranium of *Amphicyon major*

832   (Mammalia, Carnivora, Amphicyonidae) from the Miocene of Sansan (Gers, France)

833   compared to three extant carnivores *Ursus arctos*, *Panthera leo* and *Canis lupus*.

834   Geodiversitas 32, 65–106. https://doi.org/10.5252/g2010n1a2

835   Augustí, J., Antón, M., 2002. Mammoths, Sabertooths, and Hominids: 65 Million Years of

836   Mammalian Evolution in Europe. Columbia University Press, New York, 328 pp.

837   Azanza, B., Morales, J., 1994. *Tethytragus* nov. gen. et. *Gentrytragus* nov. gen. Deux

838   nouveaux Bovidés (Artiodactyla, Mammalia) du Miocène moyen. Relations

839   phylogénétiques des Bovidés anté-vallésiens. Proc. K. Ned. Akad. Wet. 97, 249–282.

840   Bachmayer, F., Młynarski, M., 1981. *Testudo kalksburgensis* Toula, 1896, eine valide

841   Schildkrötenart aus den miozänen Stranbildungen von Kalksburg bei Wein. Sitzungsber.

842   Österr. Akad. Wiss. Math.-Naturwiss. Kl. 190, 111–119.

843   Backwell, L., Steininger, C., Neveling, J., Abdala, F., Pereira, L., Mayer, E., Rossouw, L., de

844   la Peña, P., Brink, J., 2018. Holocene large mammal mass death assemblage from South

845   Africa. Quat. Int. 495, 49–63. https://doi.org/10.1016/j.quaint.2017.11.055

846   Becker, D., 2003. Paléoécologie et paléoclimats de la Molasse du Jura (Oligo-Miocène):

847   apport des Rhinocerotoidea (Mammalia) et des minéraux argileux. GeoFocus 9, 1–328.

848   Behrensmeyer, A.K., 1978. Taphonomic and ecologic information from bone weathering.

849   Paleobiol. 4, 150–162. https://doi.org/10.1017/S0094837300005820

850   Behrensmeyer, A.K., 1991. Terrestrial vertebrate accumulations. In: Allison, P.A., Briggs,

851   D.E.G. (Eds.), Taphonomy: Releasing the data locked in the fossil record. Plenum Press,

852   New York, pp. 291–335.

853   Behrensmeyer, A.K., 2007. Bonebeds through Time. In: Rogers, R.R., Eberth, A.D., Fiorillo,

854   R.A. (Eds.), Bonebeds: genesis, analysis, and paleobiological significance. University of

855   Chicago Press, Chicago, pp. 65–97.

856   Bibi, F., Güleç, E.S., 2008. Bovidae (Mammalia: Artiodactyla) from the Late Miocene of

857   Sivas, Turkey. J. Vertebr. Paleontol. 28, 501–519.

858   https://doi.org/10.1671/0272-4634(2008)28[501:BMAFTL]2.0.CO;2

859   Bimka, J., Guryča, I., Heyna, M., Holzknecht, M., Jelínková, Ž., Koukolíček, R., Králová, Z.,

860   Procházka, P., Řehánek, J., Šelle, M., Kotásek, V., Vala, Z., Valášek, S., 1983. Závěrečná

861   zpráva o hlubokém strukturním vrtu Nové Mlýny-2. MS Geofond (signature GF P051434),

862   Czech Geological Survey, Prague.

863   Böhme, M., 2003. Miocene Climatic Optimum: evidence from Lower Vertebrates of Central

864   Europe. Palaeogeogr. Palaeoclim. Palaeoecol. 195, 389–401.

865   https://doi.org/10.1016/S0031-0182(03)00367-5

866   Böhme, M., Ilg, A., Winklhofer, M., 2008. Late Miocene "washhouse" climate in Europe.

867   Earth. Planet. Sc. Lett. 275, 393–401. https://doi.org/10.1016/j.epsl.2008.09.011

868 Böhme, M., Winklhofer, M., Ilg A., 2011. Miocene precipitation in Europe: Temporal trends

869 and spatial gradients. Palaeogeogr. Palaeoclim. Palaeoecol. 304, 212–218.

870 https://doi.org/10.1016/j.palaeo.2010.09.028

871 Böhme, M., Aiglstorfer, M., Uhl, D., Kullmer, O., 2012. The antiquity of the Rhine River:

872 stratigraphic coverage of the Dinotheriensande (Eppelsheim Formation) of the Mainz

873 Basin (Germany). PLoS One 7, e36817. https://doi.org/10.1371/journal.pone.0036817

874 Brzobohatý, R., Stráník, Z., 2012. Paleogeography of the Early Badenian connection

875 between the Vienna Basin and the Carpathian Foredeep. Cent. Eur. J. Geosci. 4, 126–

876 137. https://doi.org/10.2478/s13533-011-0045-z

877 Brzobohatý, R., Nolf, D., Kroupa, O., 2007. Fish otoliths from the Middle Miocene of

878 Kienberg at Mikulov, Czech Republic, Vienna Basin: their paleoenvironmental and

879 paleogeographic significance. Bull. Inst. R. Sci. Nat. Belgique Sci. Terre 77, 167–196.

880 Březina, J., 2019. Neogenní savci z okolí Mikulova. Acta Mus. Morav. Sci. Geol. 104, 217–

881 239.

882 Buday, T., Cicha, I., Čtyroký, P., Fejfar, O., 1964. Die Stellung des Neogens der

883 Westkarpaten in der Paratethys. Cursillos Conf. Inst. Lucas Mallada 9, 109–116.

884 Calandra, I., Göhlich, U.B., Merceron, G., 2008. How could sympatric megaherbivores

885 coexist? Example of niche partitioning within a proboscidean community from the

886 Miocene of Europe. Naturwissenschaften 95, 831–838.

887 https://doi.org/10.1007/s00114-008-0391-y

888 Calandra, I., Göhlich, U.B., Merceron, G., 2010. Feeding preferences of *Gomphotherium*

889 *subtapiroideum* (Mammalia, Proboscidea) from the Miocene of Sandelzhausen (Northern

890 Alpine Foreland Basin, southern Germany) through life and geological time: Evidence

891 from dental microwear analysis. Paläontol. Z. 84, 205–215.

892 https://doi.org/10.1007/s12542-010-0054-0

893   Cerdeño, E., 1993. Étude sur *Diaceratherium aurelianense* et *Brachypotherium brachypus*

894   (Rhinocerotidae, Mammalia) du Miocène moyen de France. Bull. Mus. Natl. Hist. Nat. 4,

895   25–77.

896   Cerha, J., 1987. Zpráva o stavebně geologickém průzkumu pro PP Mikulov - Valtická -

897   Zemník. MS, Geofond (signature GF P060807). Czech Geological Survey, Prague

898   Čerňanský, A., Tóth, C., Šurka, J., 2012. Nálezy krokodíla a korytnačiek zo spodného

899   miocénu lokality Baňa Dolina vo Veľkom Krtíši (Slovensko). Acta Geol. Slovaca 4, 113–

900   123.

901   Chen, L., Lu, Y., Wu, J., Xing, F., Liu, L., Ma, Y., Rao, D., Peng, L., 2015. Sedimentary

902   facies and depositional model of shallow water delta dominated by fluvial for Chang 8 oil-

903   bearing group of Yanchang Formation in southwestern Ordos Basin, China. J. Cent. South

904   Univ. 22, 4749–4763. https://doi.org/10.1007/s11771-015-3027-3

905   Costeur, L., Guérin, C., Madriet, O., 2012. Paléoécologie et paléoenvironnement du site

906   miocène de Sansan. In: Peigné, S., Sen, S. (Eds.), Mammifères de Sansan. Mem. Mus.

907   Natl. Hist. Nat. 203, 661–693.

908   Čtyroký, P., 1989. Pannonian and Pontian at the SW margin of the Wiena Basin near

909   Mikulov. Věstn. Ústřed. Úst. Geol. 64, 257–265.

910   Čtyroký, P., 1999. Geologická mapa 1:500 000 moravské části vídeňské pánve. Zpr. Geology.

911   Výzk. Roce 1998, 88–91.

912   Čtyroký, P., Havlíček, P., Stráník, Z., Pálenský, P., 1995. Geologická a přírodovědná mapa

913   CHKO a BR Pálava 1:25 000. Český geologický ústav, Praha.

914   Čtyroký, P., Adámek, J., Brunnerová, Z., Čekan, V., Čtyroká, J., Dudek, A., Eliáš, M.,

915   Eliášová, H., havlíček, P., Hrkal, Z., Klečák, J., Kolejka, J., Molčíková, V., Novák, Z.,

916   Stráník, Z., 1990. Vysvětlivky k základní geologické mapě ČSSR 1:25 000 34–141

917   Mikulov. Ústřední ústav geologický, Praha.

918   Dasgupta, S., Buatois, L.A., Mángano, M.G., 2016. Living on the edge: evaluating the impact

919   of stress factors on animal-sediment interactions in subenvironments of a shelf-margin

920   delta, the Mayaro Formation, Trinidad. J. Sediment. Res. 86, 1034–1066.

921   https://doi.org/10.2110/jsr.2016.47

922   De Bruijn, H., Daams, R., Daxner-Höck, G., Fahlbusch, V., Ginsburg, L., Mein, P., Morales,

923   J., 1992. Report of the RCMNS working group on fossil mammals, Reisensburg 1990.

924   Newsl. Stratigr. 26, 65–118.

925   Delfino, M., Luján, À.H., Carmona, R., Alba, D.M., 2012. Revision of the extinct Pleistocene

926   tortoise *Testudo lunellensis* Almera and Bofill, 1903 from Cova de Gràcia (Barcelona,

927   Spain). Amphibia-Reptilia 33, 215–225. https://doi.org/10.1163/156853812X636466

928   DeMiguel, D., Azanza, B., Morales, J., 2011. Paleoenvironments and paleoclimate of the

929   Middle Miocene of central Spain: A reconstruction from dental wear of ruminants.

930   Palaeogeogr. Palaeoclim. Palaeoecol. 302, 452–463.

931   https://doi.org/10.1016/j.palaeo.2011.02.005

932   Domingo, L., Cuevas-González, J., Grimes, S.T., Hernández Fernández, M., López-Martínez,

933   N., 2009. Multiproxy reconstruction of the palaeoclimate and palaeoenvironment of the

934   Middle Miocene Somosaguas site (Madrid, Spain) using herbivore dental enamel.

935   Palaeogeogr. Palaeoclim. Palaeoecol. 272, 53–68.

936   https://doi.org/10.1016/j.palaeo.2008.11.006

937   Domingo, L., Koch, P.L., Grimes, S.T., Morales, J., López-Martínez, N., 2012. Isotopic

938   paleoecology of mammals and the Middle Miocene Cooling event in the Madrid Basin

939   (Spain). Palaeogeogr. Palaeoclim. Palaeoecol. 339–341, 98–113.

940   https://doi.org/10.1016/j.palaeo.2012.04.026

941   Eberth, A.D., Rogers, R.R., Fiorillo, R.A., 2007. A practical approach to the study of

942   bonebeds. In: Rogers, R.R., Eberth A.D., Fiorillo, R.A. (Eds.), Bonebeds: Genesis,

943   Analysis, and Paleobiological Significance. University of Chicago Press, Chicago, pp.

944   265–332.

945   Estes, R. 1969. Die Fauna der miozäner Spaltefüllung von Neudorf an der March (ČSSR),

946   Reptilia (Lacertilia). Sitz. Österr. Akad. Wiss., Math. Naturwiss. Klasse, 178, 77–82.

947   Fejfar, O., 1990. The Neogene vertebrate paleontology sites of Czechoslovakia: A

948   contribution to the Neogene terrestrial biostratigraphy of Europe based on rodents. In:

949   Lindsay, E.H., Fahlbusch, V., Mein, P. (Eds.), European Neogene Mammal Chronology.

950   Plenum Press, New York, pp. 211–236.

951   Francírek, M., 2018. Sedimentárně geologické studium neogenních sedimentů karpatské

952   předhlubně v oblasti Vizovických vrchů. PhD. Thesis, 103 pp., Masaryk University.

953   Gasamans, N., Luján, À.H., Pons-Monjo, G., Obradó, P., Casanovas-Vilar, I., Alba, D.M., in

954   press. The record of *Prodeinotherium* in the Iberian Peninsula: New data from the Vallès-

955   Penedès Basin. J. Mamm. Evol. https://doi.org/10.1007/s10914-021-09543-y

956   Georgalis, G.L., Joyce, W.G., 2017. A review of the fossil record of Old World turtles of the

957   clade Pan-Trionychidae. Bull. Peabody Mus. Nat. Hist. 58, 115–208.

958   https://doi.org/10.3374/014.058.0106

959   Ginsburg, L., 1961. La Faune des carnivores Miocènes de Sansan. Mem. Mus. Natl. Hist. Nat.

960   9, 1–190.

961   Ginsburg, L., Antunes M.T., 1968. *Amphicyon giganteus*, Carnassier géant du Miocene. Ann.

962   Paléontol. 54, 1–32.

963   Ginsburg, L., Chevrier, F., 2001. Les Dinothères du bassin de la Loire et l'évolution du genre

964   *Deinotherium* en France. Symbioses 5, 9–24.

965   Göhlich, U.B., 1998. Elephantoidea (Proboscidea, Mammalia) aus dem Mittel- und

966   Obermiözan der Oberen Süsswassermolasse Süddeutschlands: Odontologie und

967   Osteologie. Münch. Geowiss. Abh. A36, 1–245.

968 Göhlich, U.B., 2010. The Proboscidea (Mammalia) from the Miocene of Sandelzhausen

969   (southern Germany). Paläontol. Z. 84, 163–204.

970   https://doi.org/10.1007/s12542-010-0053-1

971 Green, J.L., Semprebon, G., Solounias, N., 2005. Reconstructing the paleodiet of Florida

972   *Mammut americanum* via low-magnification stereomicroscopy. Palaeogeogr.

973   Palaeoclimatol. Palaeoecol. 223, 34–48. https://doi.org/10.1016/j.palaeo.2005.03.026

974 Guérin C., 2012. *Anisodon grande* (Perissodactyla, Chalicotheriidae) de Sansan. In: Peigné,

975   S., Sen, S. (Eds.), Mammifères de Sansan. Mem. Mus. Natl. Hist. Nat. 203, 279–315.

976 Harzhauser, M., Piller, W.E., Mülleger, S., Grunert, P., Micheels, A., 2011. Changing

977   seasonality patterns in Central Europe from Miocene Climate Optimum to Miocene

978   Climate Transition deduced from the Crassostrea isotope archive. Glob. Planet. Change 76,

979   77–84. https://doi.org/10.1016/j.gloplacha.2010.12.003

980 Harzhauser, M., Grunert, P., Mandic, O., Lukeneder, P., García Gallardo, Á., Neubauer T.A.,

981   Carnevale G., Landau B.M., Sauer R., Strauss P., 2018. Middle and Late Badenian

982   palaeoenvironments in the northern Vienna Basin and their potential link to the Badenian

983   Salinity Crisis. Geol. Carpath. 69, 149–168. https://doi.org/10.1515/geoca-2018-0009

984 Haynes, G., 1985. Age profiles in elephant and mammoth bone assemblages. Quat. Res. 24,

985   333–345. https://doi.org/10.1016/0033-5894(85)90055-9

986 Haynes, G., 1988. Mass deaths and serial predation: Comparative taphonomic studies of

987   modern large mammal death sites. J. Archaeol. Sci. 15, 219–235.

988   https://doi.org/10.1016/0305-4403(88)90064-7

989 Haynes G., 1991. Mammoths, Mastodonts and Elephants. Biology, Behavior and the Fossil

990   Record. Cambridge University Press, Cambridge.

991 Haynes, G., 2017. Finding meaning in mammoth age profiles. Quat. Int. 443A, 65–78.

992   https://doi.org/10.1016/j.quaint.2016.04.012

993   Haynes, G., 2018. Raining more than cats and dogs: Looking back at field studies of

994   noncultural animal-bone occurrences. Quat. Int. 466B, 113–130.

995   https://doi.org/10.1016/j.quaint.2015.10.119

996   Haynes, G., Klimowicz, J., 2015. Recent elephant-carcass utilization as a basis for

997   interpreting mammoth exploitation. Quat. Int. 359–360, 19–37.

998   https://doi.org/10.1016/j.quaint.2013.12.040

999   Heckeberg, N.S., 2017. Origination of antlerogenesis. J. Morphol. 278, 182–202.

1000   https://doi.org/10.1002/jmor.20628

1001   Heissig, K., 1999. Family Rhinocerotidae. In: Rössner, G., Heissig, K. (Eds.), The Miocene

1002   Land Mammals of Europe. Dr. Friedrich Pfeil, München, pp. 175–188.

1003   Heissig, K., 2009. The early Vallesian vertebrates of Atzelsdorf (Late Miocene, Austria) 11.

1004   Rhinocerotidae and Chalicotheriidae (Perissodactyla). Ann. Nathist. Mus. Wien 111A,

1005   619–634.

1006   Heissig, K., 2012. Les Rhinocerotidae (Perissodactyla) de Sansan. In: Peigné, S., Sen, S.

1007   (Eds.), Mammifères de Sansan. Mem. Mus. Natl. Hist. Nat. 203, 317–485.

1008   Hilgen, F.J., Lourens, L.J., Van Dam, J.A., Beu, A.G., Boyes, A.F., Cooper, R.A., Krijgsman,

1009   W., Ogg, J.C., Piller, W.E., Wilson, D.S., 2012. The Neogene period. In: Gradstein, F.M.,

1010   Ogg, J.G., Schmitz, M.D., Ogg, G.M. (Eds.), The Geologic Time Scale 2012, Volume 2.

1011   Elsevier, Amsterdam, pp. 923–978.

1012   Hohenegger, J., Ćorić, S., Wagreich, M., 2014. Timing of the Middle Miocene Badenian

1013   Stage of the Central Paratethys. Geol. Carpath. 65, 55–66.

1014   https://doi.org/10.2478/geoca-2014-0004

1015   Holec, P., 1985. Finds of mastodon/Proboscidea, Mammalia/relics in Neogene and

1016   Quaternary sediments of Slovakia/ČSSR. Západn. Karp. sér. Paleontol. 10, 13–53.

1017   Hörnes, M., 1848. *Dinotherium* von Nikolsburg. Berichte über die Mitteilungen von Freunden

1018   der Naturwissenschaften in Wien 3, 160–161.

1019   Hutson, J.M., Burke, C.C., Haynes, G., 2013. Osteophagia and bone modifications by giraffe

1020   and other large ungulates. J. Archaeol. Sci. 40, 4139–4149.

1021   https://doi.org/10.1016/j.jas.2013.06.004

1022   Hünermann, K.A., 1989. Die Nashornskelette (*Aceratherium incisivum* Kaup 1832) aus dem

1023   Jungtertiär vom Höwenegg im Hegau (Südwestdeutschland). Andrias 6, 1–116.

1024   Jiříček, R., 2002. Molasový vývoj alpsko-karpatské předhlubně a vídeňské pánve. Explor.

1025   Geophys. Remote Sens. Environ. 9, 4–178.

1026   Jüttner, K., 1938. Das Neogen des unteren Thayalandes. Verhandlungen Geol. Bundesanst.

1027   32, 201–224.

1028   Jüttner, K., 1939a. Aufschlüsse als geologische Dokumente im unteren Thayalande. Jahrb.

1029   Reichsanst. Bodenforsch. Zweigstelle Wien 89B, 377–411.

1030   Jüttner, K., 1939b. Geologische Karte des Unteren Thayalandes. Mitteilungen der Reichsstelle

1031   für Bodenforschung, 1, 1. Wien.

1032   Jüttner, K., 1940. Erläuterungen zur geologischen Karte des unteren Thayalandes. Mitt.

1033   Reichsstelle Bodenforsch. 1, 1–57.

1034   Kaiser, T., 2009. *Anchitherium aurelianense* (Equidae, Mammalia): a brachydont —dirty

1035   browser in the community of herbivorous large mammals from Sandelzhausen (Miocene,

1036   Germany). Paläontol. Z. 83, 131–140. https://doi.org/10.1007/s12542-009-0002-z

1037   Kázmér, M., 2008. The Miocene Bükkábrány Fossil Forest in Hungary – field observations

1038   and project outline. Hantkeniana 6, 229–244.

1039   Koufos, G.D., 2016. Neogene and Quarternary continental biostratigraphy of grece based on

1040   mammals. Bull. Geol. Soc. Greece 50, 55–64. https://doi.org/10.12681/bgsg.11701

1041   Kováč, M., Nagymarosy, A., Holcová, K., Hudáčková, N., Zlinská, A., 2001.

1042   Paleogeography, paleoecology and eustasy: Miocene 3rd order cycles of relative sea-level

1043   changes in the Western Carpathian-North Pannonian basins. Acta Geol. Hung. 44, 1–45.

1044   Kováč, M., Andreyeva-Grigorovich, A., Bajraktarević, Z., Brzobohatý, R., Filipescu, S.,

1045   Fodor, L., Harzhauser, M., Nagymarosy, A., Oszczypko, N., Pavelić, D., Rögl, F., Saftić,

1046   B., Sliva, L., Studencka, B., 2007. Badenian evolution of the Central Paratethys Sea:

1047   paleogeography, climate and eustatic sea-level changes. Geol. Carpath. 58, 579–606.

1048   Kováč, M., Halásová, E., Hudáčková, N., Holcová, K., Hyžný, M., Jamrich, M., Ruman, A.,

1049   2018. Towards better correlation of the Central Paratethys regional time scale with the

1050   standard geological time scale of the Miocene Epoch. Geol. Carpath. 69, 3, 283–300.

1051   https://doi.org/10.1515/geoca-2018-0017

1052   Kováčová, M., Doláková N., Kováč, M., 2011. Miocene vegetation pattern and climate

1053   change in the northwestern Central Paratethys domain (Czech and Slovak Republic). Geol.

1054   Carpath. 62, 251–266. https://doi.org/10.2478/v10096-011-0020-0

1055   Kovar-Eder, J., Teodoridis, V., 2018. The Middle Miocene Central European plant record

1056   revisited; widespread subhumid sclerophyllous forests indicated. Fossil Imprint, 74, 115–

1057   134. https://doi.org/10.2478/if-2018-0009

1058   Kuklová, K., 1970. Zpráva o provedení doplňujícího hydrogeologického průzkumu.

1059   Pohořelice II–III. etapa. Lokalita Mikulov. MS, Geofond (signature GF P022573). Czech

1060   Geological Survey, Prague.

1061   Kuklová, K., 1978. Závěrečná zpráva o regionálním hydrogeologickém průzkumu neogenních

1062   uloženin jihozápadní části rajónu R 33. MS, Geofond (signature GF FZ 005709). Czech

1063   Geological Survey, Prague.

1064   Kuss, S., 1965. Revision der europäischen Amphicyoninae (Canidae, Carnivora, Mammalia)

1065   ausschliesslich der voroberstampischen Formen. Sitzungsberichte der Heidelberg

1066   Akademie der Wissenschaften, Mathematisch-naturwissenschaftliche Klasse 1, 1–168.

1067   Kvaček, Z., Böhme, M., Dvořák, Z., Konzalová, M., Mach, K., Prokop, J., Rajchl, M., 2004.

1068   Early Miocene freshwater and swamp ecosystems of the Most Basin (north Bohemia) with

1069   particular reference to the Bilina Mine section. J. Czech Geol. Soc. 49, 1–40.

1070   Kvaček, Z., Kováč, M., Kovar-Eder, J., Doláková, N., Jechorek, H., Parashiv, V., Kováčová,

1071   M., Sliva, L., 2006. Miocene evolution of landscape and vegetation in the Central

1072   Paratethys. Geol. Carpath. 57, 295–310.

1073   Lambert, W.D., 1996. The biogeography of the gomphotheriid proboscideans of North

1074   America. In: Shoshani, J., Tassy, P., (Eds.), The Proboscidea: Evolution and Palaeoecology

1075   of Elephants and Their Relatives. Oxford University Press, Oxford, pp. 143–148.

1076   Lambert, W.D., Shoshani, J., 1998. Proboscidea. In: Janis, C.M., Scott, K.M., Jacobs, L.L.

1077   (Eds.), Evolution of Tertiary Mammals of North America Volume 1: Terrestrial

1078   Carnivores, Ungulates, and Ungulate-like Mammals. Cambridge University Press,

1079   Cambridge, pp. 606–621.

1080   Lapparent de Broin F., 2000. Les Chéloniens de Sansan. In: Ginsburg, L., (Ed.), La faune

1081   Miocéne de Sansan et son environment. Mem. Mus. Nat. Hist. Nat. 183, 219–261.

1082   Luján, À.H., 2015. Les tortugues (Testudines) del Neogeni Quaternari de Catalunya (NE de la

1083   Península Ibèrica). PhD. Thesis. Universitat Autònoma de Barcelona, Barcelona, pp. 282.

1084   Luján, À.H., Delfino, M., Casanovas-Vilar, I. Alba, D.M., 2014. Taxonomy of subgenus

1085   *Temnoclemmys* Bergounioux, 1958 (Testudines: Geoemydidae: Ptychogasterinae) based on

1086   new material from the Vallès-Penedès Basin. C. R. Palevol 13, 277–295.

1087   https://doi.org/10.1016/j.crpv.2013.11.004

1088   Luján, À.H., Delfino, M., Robles, J.M., Alba, D.M., 2016. A review of the Miocene tortoise

1089   *Testudo catalaunica* Bataller, 1926 and a revised phylogeny of extinct species of genus

1090   *Testudo* (Testudines: Testudinidae). Zool. J. Linn. Soc. 178, 312–342.

1091   https://doi.org/10.1111/zoj.12414

1092   Luján, À.H., Čerňanský, A., Bonilla-Salomón, I., Březina, J., Ivanov M., in press. Fossil

1093   turtles from the early Miocene localities of Mokrá-Quarry (Burdigalian, MN4), South

1094   Moravian Region, Czechia. Geodiversitas.

1095   Marmi, J., Luján, À.H., 2012. An overview of the threatened phylogenetic diversity of living

1096   testudines based on a review of the complex evolutionary history of turtles. In: Cosgrove,

1097   M.J., Roe, S.A., (Eds.), Turtles: Anatomy, Ecology and Conservation. Nova Science

1098   Publishers, New York, pp. 117–150.

1099   Mein, P., 1975. Résultats du groupe de travail des vertébrés: Biozonation du Néogène

1100   méditerranéen à partir des mammifères. In: Senes, J. (Ed.), Report on Activity of the

1101   RCMNS Working Groups (1971–1975). Slovak Academy of Sciences, Bratislava, pp. 78–

1102   81.

1103   Mein, P., 1990. Updating of MN zones. In: Lindsay, E.H., Fahlbusch, V., Mein, P. (Eds.),

1104   European Neogene Mammal Chronology. Plenum Press, New York, pp. 73–90.

1105   Mein, P., 1999. European Miocene Mammal Biochronology. In: Rössner, G.E., Heissig, K.

1106   (Eds.), The Miocene Land Mammals of Europe. Dr. Friedrich Pfeil, München, pp. 25–38.

1107   McPherson, J.G., Shanmugam, G., Moiola, R.J., 1988. Fan deltas and braid deltas: conceptual

1108   problems. In: Nemec, W., Steel, R.J. (Eds.), Fan Deltas: Sedimentology and Tectonic

1109   Settings. Blackie, Glasgow, pp. 14–22.

1110   Miall, A.D., 1996. The geology of fluvial deposits: sedimentary facies, basin analysis and

1111   petroleum Geology. Springer-Verlag, Berlin, 582 pp.

1112   Miklas-Tempfer, P.M., 2003. The Miocene Herpetofaunas of Grund (Caudata; Chelonii,

1113   Sauria, Serpentes) and Mühlbach am Manhartsberg (Chelonii, Sauria, Amphisbaenia,

1114   Serpentes), Lower Austria. Ann. Naturhist. Mus. Wien. 104A, 195–235.

1115   Miklas-Tempfer, P.M., 2005. The Herpetofauna (Amphibia: Caudata, Anura; Reptilia:

1116   Sceroglossa) of the Upper Miocene Locality Kohfidisch (Burgenland, Austria). Beitr.

1117   Paläontol. 29, 145–253.

1118   Musil, R., 1956. Nález lebky Deinotheria na jižní Moravě. Acta Mus. Morav. Sci. Natural. 41,

1119   65–86.

1120   Nemec, W., 1990. Deltas - remarks on terminology and classification. In: Colella, A., Prior,

1121   D.B. (Eds.), Coarse-grained Deltas. Special Publication of the International Association of

1122   Sedimentologists. Blackwell, Oxford, pp. 3–12.

1123   Olariu, C., Bhattacharya, J.P., 2006. Terminal distributary channels and delta front

1124   architecture of river-dominated delta systems. J. Sediment. Res. 76, 212–233.

1125   https://doi.org/10.2110/jsr.2006.026

1126   Patočková, V., 1966. Užití vybraných základních statistických metod pro běžnou

1127   paleontologickou praxi. M.Sc. Thesis, Masaryk University, 149 pp.

1128   Pickford, M., 2013. *Conohyus simorrensis* (Lartet, 1851) (Suidae, Mammalia) from the

1129   Middle Miocene of Carpetana (Madrid, Spain). Span. J. Palaeontol. 28, 91–102.

1130   https://doi.org/10.7203/sjp.28.1.17834

1131   Pickford, M., 2016. Biochronology of European Miocene Tetraconodontinae (Suidae,

1132   Artiodactyla, Mammalia) flowing from recent revision of the Subfamily. Ann. Naturhist.

1133   Mus. Wien A 118, 175–244.

1134   Pickford, M., Laurent, Y., 2014. Valorisation of palaeontological collections: nomination of a

1135   lectotype for *Conohyus simorrensis* (Lartet, 1851), Villefranche d'Astarac, France, and

1136   description of a new genus of tetraconodont. Estud. Geol. 70, 1–28.

1137   http://dx.doi.org/10.3989/egeol.41261.262

1138   Pickford, M., Pourabrishami, Z., 2013. Deciphering Dinotheriensande deinotheriid diversity.

1139   Palaeobiodivers. Palaeoenvir. 93, 121–150. https://doi.org/10.1007/s12549-013-0115-y

1140   Postma, G., 1990. Depositional architecture and facies of river and fan deltas: a synthesis. In:

1141   Colella, A., Prior, D.B. (Eds.), Coarse-grained Deltas. Special Publication of the

1142   International Association of Sedimentologists, Blackwell, Oxford, pp. 13–27.

1143   Rogers, R.R., Kidwell, M.S., 2007. A conceptual framework for the genesis and analysis of

1144   vertebrate skeletal concentrations, in: Rogers, R.R., Eberth, A.D., Fiorillo, R.A. (Eds.),

1145   Bonebeds: genesis, analysis, and paleobiological significance. University of Chicago Press,

1146   Chicago, pp. 1–63.

1147   Rotgers, C., Alba, D.M., Robles, J.M., Casanovas-Vilar, I., Galindo, J., Bertó, J.V., Moyà-

1148   Solà, S., 2011. A new species of *Anchitherium* (Equidae: Anchitheriinae) from the Middle

1149   Miocene of Abocador de Can Mata (Vallès-Penedès Basin, NE Iberian Peninsula). C. R.

1150   Palevol 10, 567–576. https://doi.org/10.1016/j.crpv.2011.06.003

1151   Rössner, G.E., 2010. Systematics and palaeoecology of Ruminantia (Artiodactyla, Mammalia)

1152   from the Miocene of Sandelzhausen (southern Germany, Northern Alpine Foreland Basin).

1153   Paläontol. Z. 84, 123–162. https://doi.org/10.1007/s12542-010-0052-2

1154   Rössner, G.E, Costeur, L., Scheyer, T.M., 2021. Antiquity and fundamental processes of the

1155   antler cycle in Cervidae (Mammalia). Sci. Nat. 108, 1–24. https://doi.org/10.1007/s00114-

1156   020-01713-x

1157   Rzehak, A., 1922. Das Mährische Tertiar. vol. 3. Státní Geologický Ústav Československé

1158   Republiky. Prague, 51 pp.

1159   Sabol, M., Holec, P., 2002. Temporal and spatial distribution of Miocene mammals in the

1160   Western Carpathians. Geol. Carpath. 53, 269–279.

1161   Sabol, M., Kováč, M., 2006. Badenian Palaeoenvironment, Faunal Succession and

1162   Biostratigraphy: A Case Study from Northern Vienna Basin, Devínska Nova Ves-Bonanza

1163   site (Western Carpathians, Slovakia). Beitr. Palaont. 30, 415–425.

1164   Schulz, E., Fahlke, J.M., Merceron, G., Kaiser, T.M., 2007. Feeding ecology of the

1165   Chalicotheriidae (Mammalia, Perissodactyla, Ancylopoda). Results from dental micro- and

1166   mesowear analyses. Verhandlung. Naturwiss. Ver. Hambg. 43, 5–32.

1167   Seitl, L., 1985. Fauna mastodontů (Proboscidea, Mammalia) moravské části vídeňské pánve.

1168   Čas. Morav. Muz. 70, 71–94.

1169   Siliceo, G., Morales, J., Antón, M., Salesa, M.J., 2020. New fossils of Amphicyonidae

1170   (Carnivora) from the middle Miocene (MN6) site of Carpetana (Madrid, Spain).

1171   Geodiversitas 42, 223–238. https://doi.org/10.5252/geodiversitas2020v42a15

1172   Steininger, F.F., 1999. Chronostratigraphy, Geochronology and Biochronology of the

1173   Miocene 'European Land Mammal Mega-Zones' (ELMMZ) and the Miocene 'Mammal-

1174   Zones (MN-Zones)'. In: Rössner, G.E., Heissig, K. (Eds.), The Miocene Land Mammals of

1175   Europe. Dr. Friedrich Pfeil, München, pp. 9–24.

1176   Stejskal, J., 1934. Geologická stavba Pavlovských vrchů na jižní Moravě. I. Stratigrafie.

1177   Věstn. Státního Geolo. Ústavu Českoslov. Repub. 10, 199–209.

1178   Stráník Z., Čtyroký, P., Havlíček, P., 1999. Geologická minulost Pavlovských vrchů. Sborník

1179   Geol. Věd. Geol. 49, 5–32.

1180   Tassy, P., 1977. Découverte de *Zygolophodon turicensis* (Schinz) (Proboscidea, Mammalia)

1181   au lieu-dit Malartic à Simorre, Gers (Vindobonien moyen); implications paléoécologiques

1182   et biostratigraphiques. Geobios 10, 655−669.

1183   https://doi.org/10.1016/S0016-6995(77)80045-4

1184   Tassy, P., 1996. Growth and sexual dimorphism among Miocene elephantoids: the example of

1185   *Gomphotherium angustidens*. In: Shoshani, J., Tassy, P., (Eds.), The Proboscidea:

1186   Evolution and Palaeoecology of Elephants and Their Relatives. Oxford University Press,

1187   Oxford, pp. 92–100.

1188   Tassy, P., 2013. L'anatomie cranio-mandibulaire de *Gomphotherium angustidens* (Cuvier,

1189   1817) (Proboscidea, Mammalia): données issues du gisement d'En Péjouan (Miocène

1190   moyen du Gers, France). Geodiversitas 35, 377–445. https://doi.org/10.5252/g2013n2a6

1191   Tassy, P., 2014. L'odontologie de *Gomphotherium angustidens* (Cuvier, 1817) d'En Péjouan

1192   (Miocène moyen du Gers, France). Geodiversitas 36, 35–115.

1193   https://doi.org/10.5252/g2014n1a2

1194   Thenius, E. 1948. Zur Kenntnis der fossilen Hirsche des Wiener Beckens, unter besonderer

1195   Berücksichtigung ihrer stratigraphischen Bedeutung. Ann. Nat. Hist. Mus. Wien. 56, 262–

1196   308.

1197   Thenius, E., 1951. *Gazella* cf. *deperdita* aus dem mitteleuropaischen Vindobonien und das

1198   Auftreten der Hipparionfauna. Eclogae Geol. Helv. 44, 381–394.

1199   Thenius, E., 1959. Tertiär. II: Wirbeltierfaunen. Handbuch der Stratigraphischen Geologie.

1200   Ferdinand Enke Verlag, Stuttgart.

1201   Thenius, E., 1979. Zur systematischen Stellung und Verbreitung von "*Gazella*" *stehlini*

1202   (Bovidae, Mammalia) aus dem Miozän Europas. Anz. Österr. Akad. Wiss. Math.-

1203   Naturwiss. Kl. 116, 9–13.

1204   Tobien, H., 1973. On the evolution of mastodonts (Proboscidea, Mammalia). Part 1: The

1205   bunodont trilophodont groups. Hess. Landesamt Bodenforsch. 101, 202–276.

1206   Tobien, H., 1975. The structure of the mastodont molar (Proboscidea, Mammalia). Part 2: The

1207   zygodont and zygobunodont patterns. Mainz. Geowiss. Mitt. 4, 195–233.

1208   Tobien H., 1996: Evolution of zygodons with emphasis on dentition. In: Shoshani, J., Tassy,

1209   P. (Eds.), The Proboscidea. Evolution and Paleoecology of Elephants and Their Relatives.

1210   Oxford University Press, Oxford, pp. 335–348.

1211   Toula, F., 1896. Ueber neue Wirbelthierreste aus dem Tertiär Oesterreichs und Rumeliens. Z.

1212   Deutsch. Geol. Ges. 48, 915–924.

1213   Tütken, T, Vennemann, T.W., Janz, H., Heizmann, E.P.J., 2006. Palaeoenvironment and

1214   palaeoclimate of the Middle Miocene lake in the Steinheim basin, SW Germany: A

1215   reconstruction from C, O, and Sr isotopes of fossil remains. Palaeogeogr. Palaeoclim.

1216   Palaeoecol. 241, 457–491. https://doi.org/10.1016/j.palaeo.2006.04.007

1217   Tütken, T., Vennemann, T., 2009. Stable isotope ecology of Miocene large mammals from

1218   Sandelzhausen, southern Germany. Paläontol. Z. 83, 207–226.

1219   https://doi.org/10.1007/s12542-009-0011-y

1220   van der Made, J., 1989. A *Conohyus*-lineage (Suidae, Artiodactyla) from the Miocene of

1221   Europe. Rev. Esp. Paleontol. 4, 19–28.

1222   van der Made, J., 2020. The Suoidea from the Middle Miocene of Gračanica (Bugojno Basin,

1223   Bosnia and Herzegovina)—evolution, taxononomy, and biostratigraphy. Palaeobiodivers.

1224   Palaeoenviron. 100, 321–349. https://doi.org/10.1007/s12549-020-00420-9

1225   van der Made, J., Salesa, M. J., 2004. Early remains of the pig *Conohyus simorrensis* from the

1226   Middle Aragonian of Somosaguas near Madrid - Its dispersal into Europe and evolution.

1227   N. Jb. Geol. Paläont. Abh. 233, 153–168. https://doi.org/10.1127/njgpa/233/2004/153

1228   Viranta, S., 1996. European Miocene Amphicyonidae: taxonomy, systematics and ecology.

1229   Acta Zool. Fenn. 204, 1–61.

1230   Vitek, N.S., Joyce, W.G., 2015. A review of the fossil record of New World turtles of the

1231   clade Pan-Trionychidae. Bull. Peabody Mus. Nat. Hist. 56, 185–244.

1232   https://doi.org/10.3374/014.058.0106

1233   Zapfe, H., 1949. Eine mittelmiozäne Säugetierfauna aus einer Spaltenfüllung bei Neudorf an

1234   der March (CSR). Sitz. Österr. Akad. Wiss., Math. Naturwiss. Klasse. 173–181.

1235   Zapfe, H., 1954. Die Fauna der miozänen Spaltenfüllung von Neudorf a. d. March (CSR.) –

1236   Proboscidea. Sitz. Österr. Akad. Wiss., Math. Naturwiss. Klasse, 163, 71–87.

1237   Zapfe, H., 1979. *Chalicotherium grande* (Blainv.) aus der miozänen Spaltenfüllung von

1238   Neudorf an der March (Děvinská Nová Ves), Tschechoslowakei. N. Denkschr. Naturhist.

1239   Mus. Wien 2, 1–284.

1240   Zapfe, H., 1993. Die Fauna der miozänen Spaltenfüllung von Neudorf an der March

1241   (Slowakei). Palaeomerycidae. Sitz. Österr. Akad. Wiss., Math. Naturwiss. Klasse. 200, 1–

1242   10, 89–136.

1243   Zhang, L., Bao, Z., Lin, Y., Chen, Y., Lin, X., Dou, L., Kong, B., 2017. Genetic types and

1244   sedimentary model of sandbodies in a shallow-water delta: A case study of the first

1245   Member of Cretaceous Yaojia Formation in Qian'an area, south of Songliao Basin, NE

1246   China. Pet. Explor. Dev. 44, 770–779. https://doi.org/10.1016/S1876-3804(17)30087-3

1247   Zhu, X., Li, S., Wu, D., Zhu, S., Dong, Y., Zhao, D., Wang, X., Zhang, Q., 2017. Sedimentary

1248   characteristics of shallow-water braided delta of the Jurassic, Junggar basin, Western

1249   China. Journal of Petroleum Science and Engineering 149, 591–602.

1250   https://doi.org/10.1016/j.petrol.2016.10.054

Figure captions

Fig. 1. A: Simplified geological map of Central Europe (A: Austria, CZ: Czech Republic, G:

Germany, H: Hungary, PL: Poland, SK: Slovakia). B: Geological map of Mikulov area where

the location of Czujan's sandpit is denoted by an asterisk (based on Jüttner, 1939b; Čtyroký et

al., 1995).

Fig. 2. Geological cross sections through the area of Czujan's sandpit reconstructed from drill

cores and boreholes: HV1 and HJ1 (Kuklová, 1970, 1978); PV1 and PV3 (Seitl, 1985); S164-

180 (Cerha, 1987). The red line indicates the border between successive upper Badenian

substages Wielician and Kosovian according to the borehole NM2 (Bimka et al., 1983).

Fig. 3. Composite stratigraphic log of the Hrušky Formation in the studied area, including the

fossil content recovered from the borehole samples (Kuklová, 1970, 1978; Seitl, 1985; Cerha,

1987) and stratigraphic boundary between successive upper Badenian substages Wielician

and Kosovian in Nové Mlýny 2 borehole (Bimka et al., 1983).

Fig. 4. Photographs taken by R. Musil in 1964 showing the uppermost part of the Hrušky

Formation. Facies association 3 (FA3, Kosovian, modified with lines indicating the

sedimentary architecture). A: sequence of two sedimentary units (St, SGt and Sh, SGh). B:

sequence of two sedimentary units (Sp facies and Sl, Gl). The irregularity of the originally

horizontally placed clay body is caused by a partial slide of the wall. Original in photoarchive

of the Department of Geology and Paleontology, MZM; colored lines are explained in the

text.

1276 **Fig. 5**. Vertebrate remains from Czujan's sandpit. A: Trionychidae indet., costal plate (PIUW-

1277 8X1939) in dorsal view. B–C: *Testudo* (*Chersine*) *kalksburgensis*, carapace and plastron

1278 (Ot7875) in dorsal (B) and visceral (C) views. D: *Prodeinotherium* cf. *bavaricum*, left M3

1279 (Ot7526), in oclusal view, E: *Zygolophodon turicensis*, right M3 (Ot7541), in oclusal view.

1280 F–G: *Gomphotherium angustidens*, right M2 (Ot7524) in (F) oclusal view; right I2 (Ot7505)

1281 in (G) lateral view. H: *Anisodon grande*, left fourth metacarpal (Ot7766) in lateral view. I:

1282 *Hoploaceratherium* sp., right tibia (Ot7749) in dorsal view. J–L: *Brachypotherium brachypus*,

1283 left tibia (Ot7752) in (J) dorsal view; right incisor (Ot7700) in (K) labial view; left maxillary

1284 fragment with M2–M3 (Ot7752) in (L) oclusal view. M: *Anchitherium* sp., right maxillary

1285 fragment with M1–M2 (Ot7765) in oclusal view. N–O: *Tethytragus stehlini*, frontoparietal

1286 with horn cores (Ot7786) in anterior (N) and left lateral (O) views. P: Palaeomerycidae indet.,

1287 right mandibular fragment with m2–m3 (Ot7773) in oclusal view. Q: *Heteroprox larteti*,

1288 partial antler (Ot7771) in side view. R: cf. *Retroporcus matritensis*, right (with m3) and left

1289 (with m1) mandibular fragments (RMM P11) in oclusal view. S–T: *Amphicyon* cf. *major*,

1290 partial left canine (Ot7814) in (S) lingual view; left calcaneus (Ot7815) in (T) proximal view.

1291

1292 **Fig. 6.** Taphonomic features of fossil vertebrate remains from Czujan's sandpit. A–B:

1293 Proboscidean right (Ot7596) and left (Ot7599) humerus from a single individual in (A–B)

1294 cranial views. C: Proboscidea indet., atlas (Ot7545) and axis (Ot7547) in anatomical

1295 articulation, in dorsal view. D: *Hoploaceratherium* sp., radius (Ot7738) and ulna (Ot7829) in

1296 anatomical articulation, in distal view. E: Artiodactyla indet. (small size), tibia (Ot7810) and

1297 astragalus (Ot7808) in anatomical articulation, in plantar view. F: Proboscidea indet., right

1298 femur (Ot7647) with unfused distal epiphysis (Ot7650), in medial view. G: Right posterior

1299 carapace fragment with well preserved growth scute lines (Ot7877) in lateral view. H–I:

1300 Rhinocerotidae indet., comparison of a well preserved radius (Ot7736) with a deformed

partial radius (Ot7737) as a possible result of trampling, in (H–I) caudal views. J: *Brachypotherium brachypus*, cracks in distal head of humerus (Ot7720), in caudal view. K–L: Proboscidea indet., proximal head of humerus (Ot7646) with gnawing traces of a large carnivore, in proximal (K) and caudal (L) views. M: Proboscidea indet., detail of gnawing traces of on the tip of tusk (Ot7483) possibly produced by a small rodent. N: *Isurus* sp., partial tooth (Ot7870), in labial view. O: wood fragment (Ot7871).

Fig 7. Stratigraphic distribution of the studied taxa in Central Europe. Age boundaries for the Badenian stage follow Kováč et al. (2018). Modified MN zonation in Western and Southwestern Europe follows Hilgen et al. (2012), Central European MN zonation modified according to Steininger (1999), Becker (2003) and Hilgen et al. (2012). The taxa ranges and ages of localities are based on various sources (see Supplementary Information).

Fig. 8. Paleoenvironments derived for Czujan's sandpit taxa. Taxa silhouettes are not in scale: 1) *Zygolophodon turicensis*; 2) *Heteroprox larteti*; 3) *Anisodon grande*; 4) Palaeomerycidae; 5) *Tethytragus stehlini* ; 6) *Amphicyon major*; 7) *Prodeinotherium bavaricum*; 8) *Brachypotherium brachypus*; 9) *Gomphotherium angustidens*; 10) *Hoploaceratherium*; 11) *Anchitherium* sp.; 12) *Retroporcus matritensis*; 13) *Testudo kalksburgensis*.

Table captions

Table 1 Comparison of minimum numbers of individuals (MNI) recorded at Czujan's sandpit with recent mass death sites reported during drought in Zimbabwe (Haynes, 1988, counted in 1986).

1325   **Table 2** Age profile of the studied proboscideans (*Zygolophodon turicensis* and

1326   *Gomphotherium angustidens*) from Czujan's sandpit. Dental ages follow Tassy (1996, 2013,

1327   2014), whereas ontogenetic age and age categories follow Haynes (2017).

1328

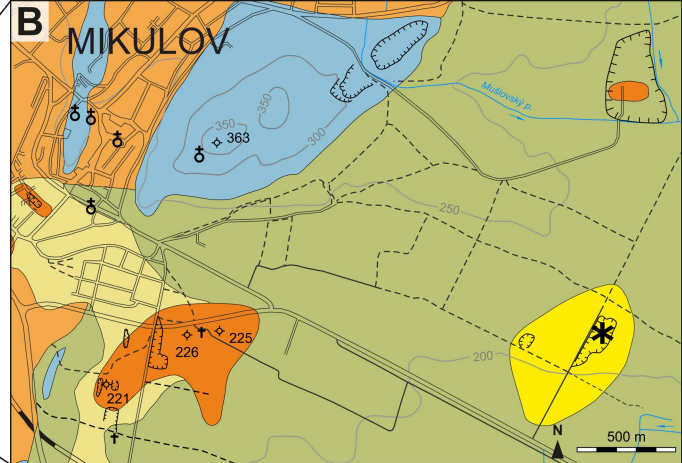1329   **Supplementary material**

1330   SUPPLEMENTARY TABLE 1
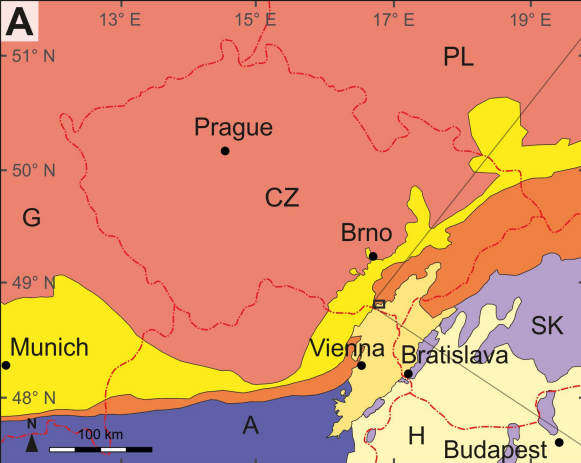
1331   List of studied material with distribution of skeletal elements for each determined taxa.
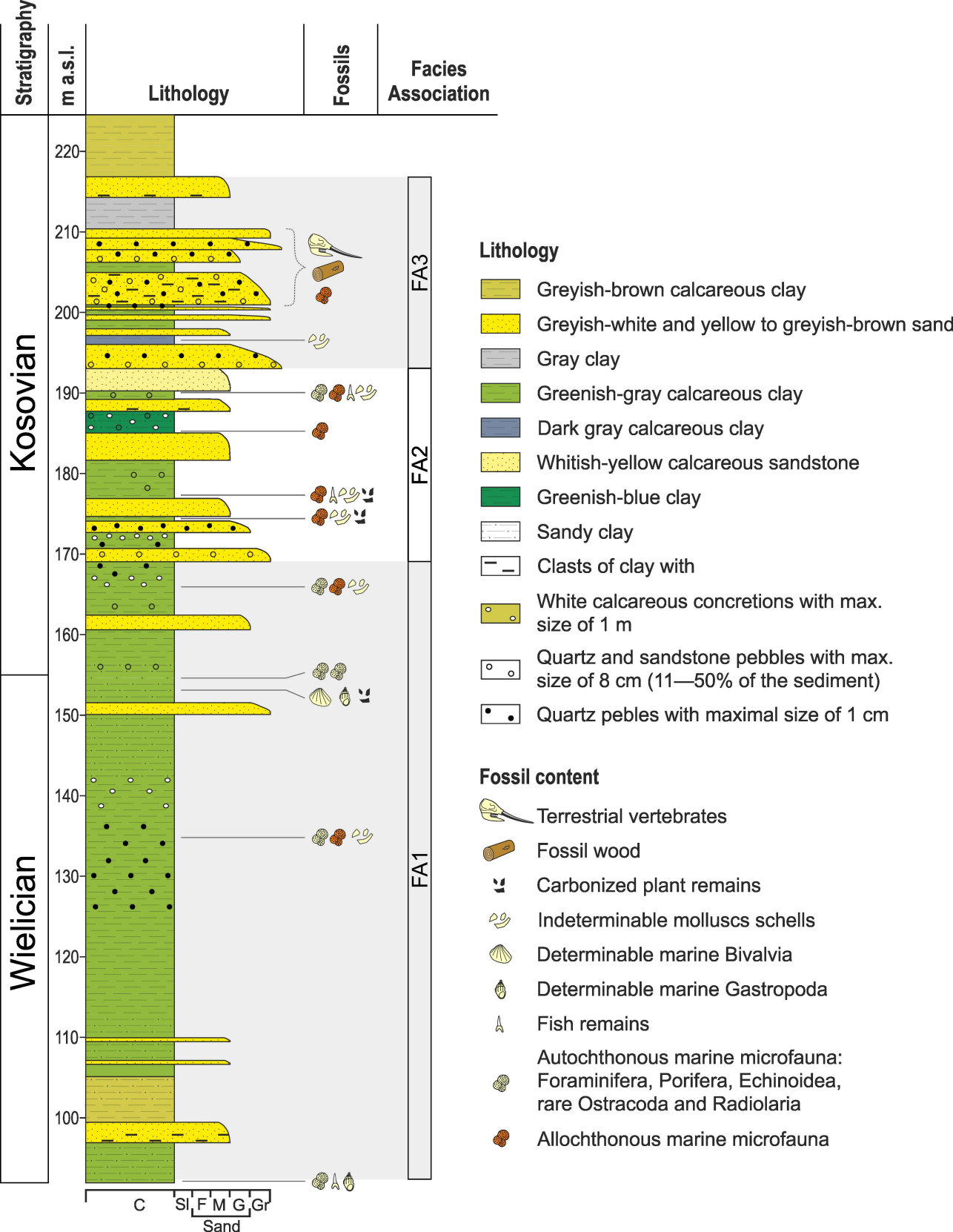
1332

1333   SUPPLEMENTARY INFORMATION.

1334   List of well dated Neogene localities in Central Europe with the occurrence of the taxa

1335   recorded at Czujan's sandpit. Countries are given in capital letters and the name of the locality
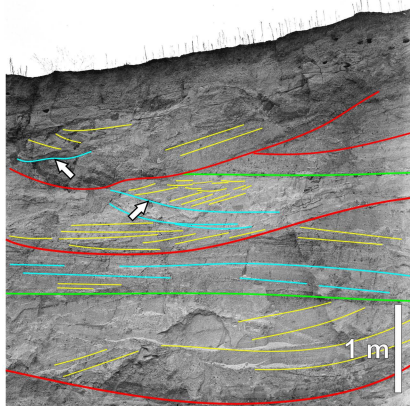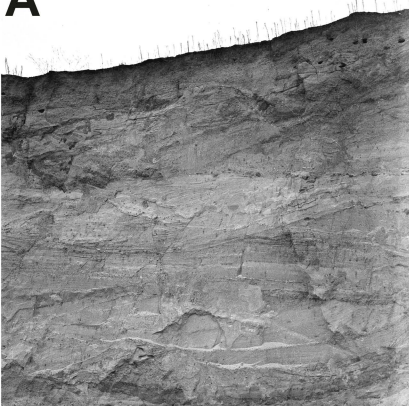
1336   is in bold.

1337

A

51° N
13° E · 15° E · 17° E · 19° E

PL

Prague ·

50° N

CZ

G

Brno ·

49° N

Munich ·

Vienna · Bratislava · SK

48° N

A

H

Budapest

N
100 km

B

MIKULOV

Mikulovský p.

350 · 350 · 300
363 ·

250

226 · 225

221

200

N
500 m

	Danube Basin
	Vienna Basin
	Carpathian Foredeep and North Alpine Foreland Basins
	External nappe-group of the Western Carpathians
	Alps
	Central Western Carpathians
	Bohemian Massif
✳	Czujan's sandpit

	Valtice Beds (upper Pannonian–?Pontian): sandy gravels
	Bzenec Formation (Pannonian): sands, siltstones (rare gravels)
	Hrušky Formation (upper Badenian): sands and gravels
	Hrušky Formation (middle-upper Badenian): calcareous clays and silts, locally calcareous sands and algal limestones
	Ždánice Unit (Oligocene-Miocene): claystones, sandstones and conglomerates
	Ždánice Unit (Jurassic-Cretaceous): limestones and marlstones
🔲	Maximum dimension of the abandoned or leveled mining sites

A

B

Legend:
- St, SGt facies co-set
- Sh, SGh facies co-set
- Clay intraclast
- Sl, Gl facies co-set
- Sp facies co-set
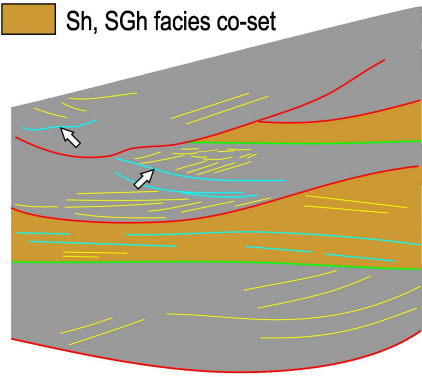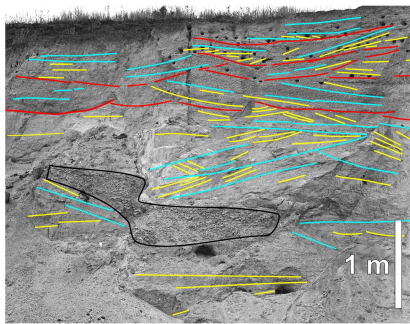
1 m

Figure with labeled specimens. Panel C labels: Atlas, Axis. Panel D labels: Radius, Ulna. Panel E labels: Tibia, Astragalus. Panel F label: Unfused epiphyseal line.

Scale bars: A, B — 5 cm; C — 5 cm; D — 2 cm; E — 2 cm; F — 10 cm; G — 2 cm; H, I — 5 cm; J — 2 cm; K — 2 cm; L — 2 cm; M — 2 cm; N — 1 cm; O — 2 cm.
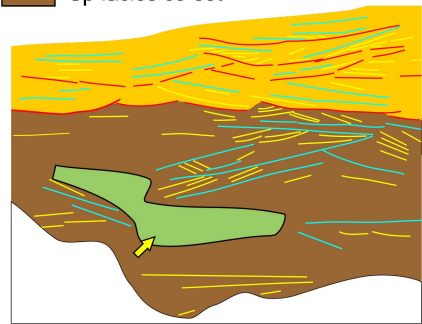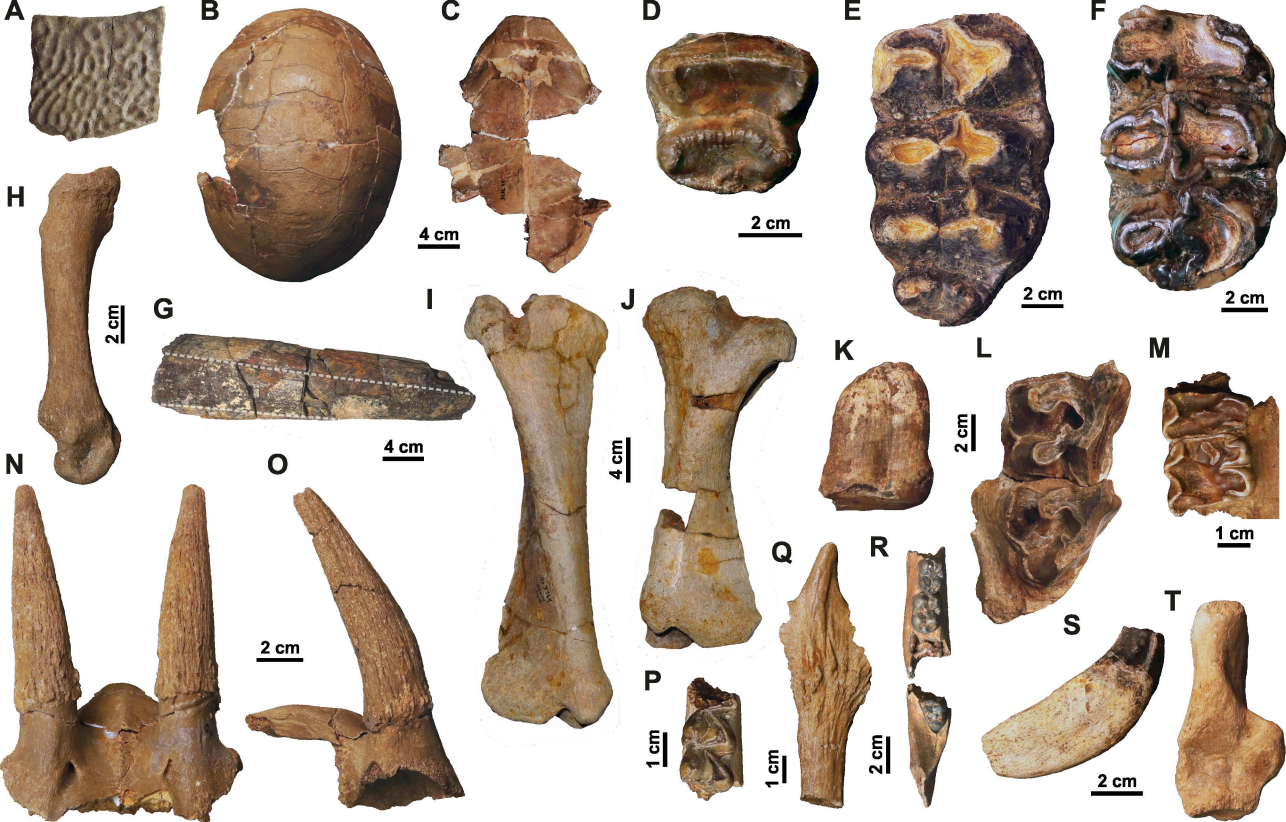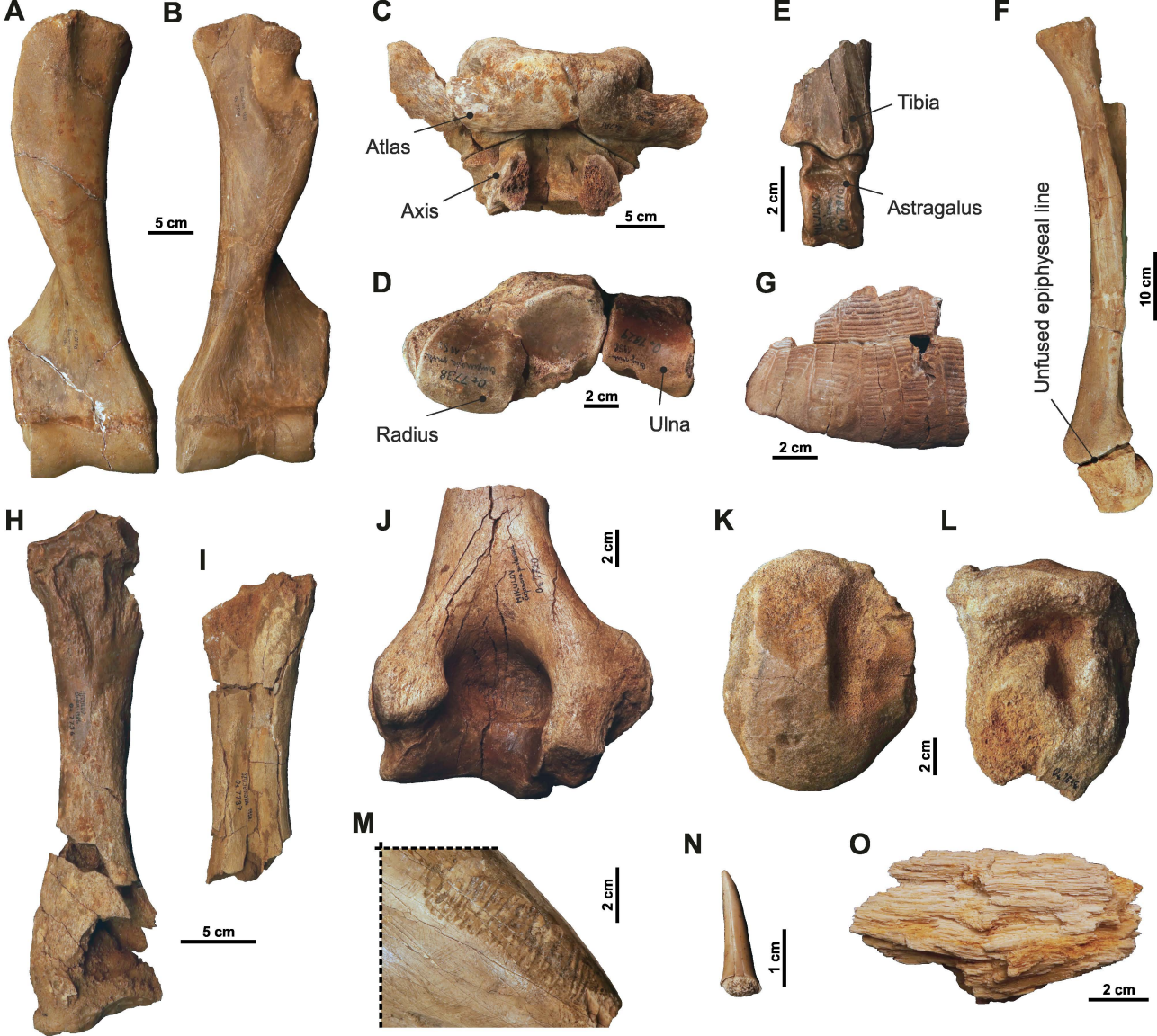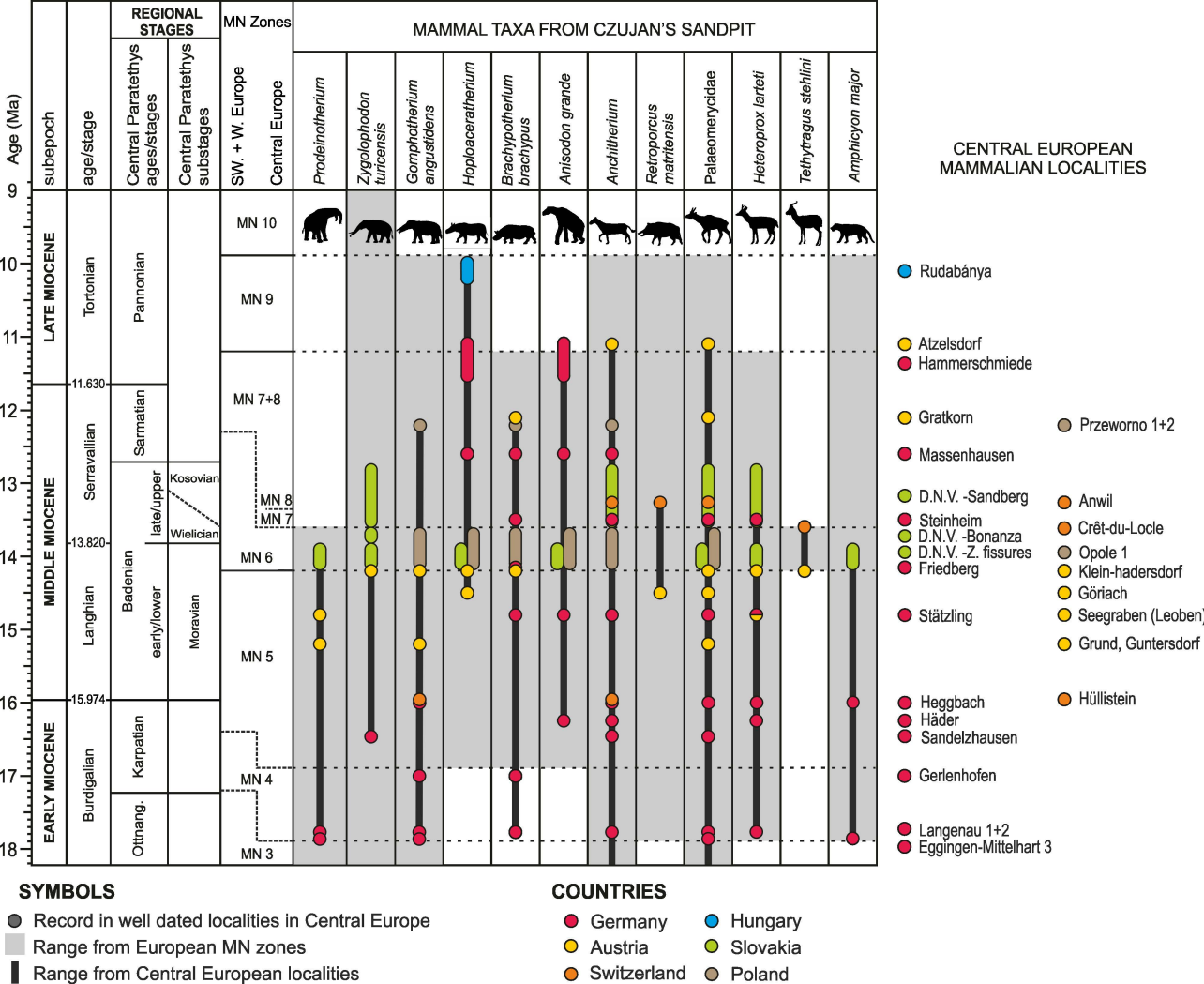
Closed environment (forest)
1 2

Open environment (woodland)

↓

Unspecified woodland
3 4 2 5 6

Closed woodland
7 1 8

Open woodland
9 10 11 12 13
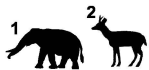
Open environment (grass dominated)
9 11 5 13

11%
16%
26%
68%
21%
26%

Table 1 Comparison of minimum numbers of individuals (MNI) recorded at Czujan's sandpit with recent mass death sites reported during drought in Zimbabwe (Haynes, 1988, counted in 1986).

Taxon	Czujan's sandpit	Shabi Shabi	Lememba	Shkawanki	Nehimba
Proboscidea	21	45	21	8	4
Non-equid Perissodactyla	7	-	-	-	-
Equidae	1	2	2	-	-
Non-bovid Ruminantia	4	-	3	1	-
Bovidae	11	11	8	1	2
Suidae	1	-	-	1	1
Carnivora	1	2	2	-	-
Aves	-	5	1	-	-
Testudines	4	4	-	-	1
Total MNIs	50	69	37	11	8
Taxa represented	14	13	8	4	5

Table 2 Age profile of studied proboscideans (*Zygolophodon turicensis* and *Gomphotherium angustidens*) from Czujan's sandpit. Dental ages follow Tassy (1996, 2013, 2014), whereas ontogenetic age follow Haynes (2017).

Dental ages	MNI		Approximate age (years)
	Zygolophodon turicensis	*Gomphotherium angustidens*	
I-II.			0–1
III.	1		1–1.5
IV-VI.			1.5–5.5
VII.	1		5.5–7
VIII-IX.			7–10
X.	1		10–13
XI-XII.			13–18
XIII.	1		18–20
XIV.	3	1	20–22
XV.	2		22–24
XVI.	4		24–27
XVII.	1		27–28
XVIII-XIX.			28–32
XX.	2	1	32–35
XXI.			35–37
XXII.		1	37–42

List of well dated Neogene localities in Central Europe with the occurrence of the taxa recorded at Czujan's sandpit. Countries are given in capital letters and the name of the locality is in bold.

AUSTRIA

Grund

Age: ~15.2 Ma (Daxner-Höck et al., 2004)

Taxa:

Locality	Supraspecific taxa	Species	References
Grund	Proboscidea	*Prodeinotherium bavaricum*	Daxner-Höck et al. (2004)
Grund	Palaeomerycidae	*Palaeomeryx eminens*	Daxner-Höck et al. (2004)

Guntersdorf

Age: ~15.2 Ma (Daxner-Höck et al., 2004)

Taxa:

Locality	Supraspecific taxa	Species	References
Guntersdorf	Proboscidea	*Gomphotherium angustidens*	Daxner-Höck et al. (2004)

Seegraben near Leoben

Age: 14.8 Ma (Aiglstorfer et al., 2014a)

Taxa:

Locality	Supraspecific taxa	Species	References
Seegraben	Proboscidea	*Prodeinotherium bavaricum*	Aiglstorfer et al. (2014a)
Seegraben	Cervidae	*Heteroprox larteti*	Aiglstorfer et al. (2014a)

Göriach

Age: ~14.5 Ma (Aiglstorfer et al., 2014a)

22   Taxa:

Locality	Supraspecific taxa	Species	References
Göriach	Rhinocerotidae	*Hoploaceratherium tetradactylum*	Heissig (2012)
Göriach	Palaeomerycidae	*Ampelomeryx magnus*	Astibia (2012)
Göriach	Suidae	*Retroporcus matritensis*	Pickford and Laurent (2014)

23

Klein-hadersdorf

25   Age: ~14.2 Ma (Böhme et al., 2012a)

26   Taxa:

Locality	Supraspecific taxa	Species	References
Klein-hadersdorf	Proboscidea	*Gomphotherium angustidens*	Thenius (1948)
Klein-hadersdorf	Proboscidea	*Zygolophodon turicensis*	Thenius (1948)
Klein-hadersdorf	Rhinocerotidae	*Hoploaceratherium* cf. *tetradactylum*	Thenius (1948)
Klein-hadersdorf	Rhinocerotidae	*Brachypotherium brachypus*	Thenius (1948)
Klein-hadersdorf	Palaeomerycidae	*Palaeomeryx eminens*	Thenius (1948)
Klein-hadersdorf	Cervidae	*Heteroprox larteti*	Thenius (1948)
Klein-hadersdorf	Bovidae	*Tethytragus stehlini*	Thenius (1951)

27

Gratkorn

29   Age: 12.2–12.0 Ma (Gross et al., 2014)

30   Taxa:

Locality	Supraspecific taxa	Species	References
Gratkorn	Rhinocerotidae	*Brachypotherium brachypus*	Gross et al. (2014)
Gratkorn	Palaeomerycidae	Palaeomerycidae indet.	Aiglstorfer et al. (2014a)

31

SLOVAKIA

Devínská Nová Ves–Zapfe's fissures

34   Age: lower part of MN6, 14.5–13.82 (Fejfar, 1990)

35   Taxa:

Site	Supraspecific taxa	Species	References
D.N.V. –Zapfe's fissures	Proboscidea	*Prodeinotherium bavaricum*	Sabol and Holec (2002)
D.N.V. –Zapfe's	Proboscidea	*Zygolophodon turicensis*	Sabol and Holec (2002)

Site	Supraspecific taxa	Species	References
fissures			
D.N.V. –Zapfe's fissures	Rhinocerotidae	*Hoploaceratherium* cf. *tetradactylum*	Sabol and Holec (2002)
D.N.V. –Zapfe's fissures	Chalicotheriidae	*Anisodon grande*	Sabol and Holec (2002)
D.N.V. –Zapfe's fissures	Cervidae	*Heteroprox larteti*	Sabol and Holec (2002)
D.N.V. –Zapfe's fissures	Palaeomerycidae	*Palaeomeryx magnus*	Sabol and Holec (2002)
D.N.V. –Zapfe's fissures	Carnivora	*Amphicyon major*	Sabol and Holec (2002)

36

37 **Devínská Nová Ves–Bonanza**

38 Age: late Badenian, 13.82–13.60 Ma (Sabol and Kováč 2006; Ivanov, in press)

39 Taxa:

Site	Supraspecific taxa	Species	References
D.N.V. – Bonanza	Proboscidea	*Zygolophodon turicensis*	Sabol and Kováč (2006)

40

41 **Devínská Nová Ves–Sandberg**

42 Age: late Badenian, 13.60–13.1 Ma (Hyžný et al., 2012)

43 Taxa:

Site	Supraspecific taxa	Species	References
D.N.V. – Sandberg	Proboscidea	*Zygolophodon turicensis*	Sabol and Holec (2002)
D.N.V. – Sandberg	Equidae	*Anchitherium aurelianense*	Sabol and Holec (2002)
D.N.V. – Sandberg	Palaeomerycidae	*Palaeomeryx kaupi*	Sabol and Holec (2002)
D.N.V. – Sandberg	Cervidae	*Heteroprox larteti*	Sabol and Holec (2002)

44

45 **SWITZERLAND**

46 **Hüllistein**

47 Age: 15.9–16.0 Ma (Aiglstorfer et al., 2014b)

48

49 Taxa:

Locality	Supraspecific taxa	Species	References
Hüllistein	Proboscidea	*Gomphotherium angustidens*	Bollinger (1992)
Hüllistein	Equidae	*Anchitherium aurelianense*	Bollinger (1992)

50

Crêt-du-Locle

51

52 Age: ~13.6 Ma (van der Made, 2012)

53 Taxa:

Locality	Supraspecific taxa	Species	References
Crêt du Locle	Bovidae	*Tethytragus stehlini*	Thenius (1951)

54

Anwil

55

56 Age:13.37–13.17 Ma (Böhme et al., 2008)

57 Taxa:

Locality	Supraspecific taxa	Species	References
Anwil	Equidae	*Anchitherium aurelianense*	Engesser (1972)
Anwil	Palaeomerycidae	*Palaeomeryx* sp.	Engesser (1972)
Anwil	Suidae	*Retroporcus matritensis*	Pickford and Laurent (2014)

58

HUNGARY

59

Rudabánya

60

61 Age: 10.3–9.9 Ma (Böhme et al., 2008)

62 Taxa:

Locality	Supraspecific taxa	Species	References
Rudabánya	Rhinocerotidae	*Hoploaceratherium belvederense*	Heissig (2005)

63

POLAND

64

Opole 1

65

66 Age: 14.5–13.7 Ma (Harzhauser and Neubauer, 2018)

67 Taxa:

Site	Supraspecific taxa	Species	References

Opole 1	Proboscidea	*Gomphotherium angustidens*	Kowalski (1990)
Opole 1	Rhinocerotidae	*Hoploaceratherium tetradactylum*	Kowalski (1990)
Opole 1	Rhinocerotidae	*Brachypotherium brachypus*	Kowalski (1990)
Opole 1	Chalicotheriidae	*Anisodon grande*	Kowalski (1990)
Opole 1	Equidae	*Anchitherium aurelianense*	Kowalski (1990)
Opole 1	Palaeomerycidae	*Palaeomeryx eminens*	Kowalski (1990)

68

Przeworno (1+2)

70 Age: ~12.2 Ma (Aiglstorfer et al., 2014b)

71 Taxa:

Site	Supraspecific taxa	Species	References
Przeworno (1+2)	Proboscidea	*Gomphotherium angustidens*	Kowalski (1990)
Przeworno (1+2)	Rhinocerotidae	*Brachypotherium brachypus*	Kowalski (1990)
Przeworno (1+2)	Equidae	*Anchitherium aurelianense*	Kowalski (1990)

72

GERMANY

Eggingen-Mittelhart 3

75 Age: 17.9–17.85 Ma (Böhme et al., 2012b)

76 Taxa:

Site	Supraspecific taxa	Species	References
Eggingen – Mittelhart 3	Proboscidea	*Prodeinotherium bavaricum*	Sach and Heizmann (2001)
Eggingen – Mittelhart 3	Proboscidea	*Gomphotherium angustidens*	Sach and Heizmann (2001)
Eggingen – Mittelhart 3	Palaeomerycidae	*Palaeomeryx kaupi*	Sach and Heizmann (2001)
Eggingen – Mittelhart 3	Carnivora	*Amphicyon* cf. *major*	Sach and Heizmann (2001)

77

Langenau

79 Age: 17.8–17.75 Ma (Böhme et al., 2012b)

80 Taxa from:

Site	Supraspecific taxa	Species	References
Langenau 1	Proboscidea	*Prodeinotherium bavaricum*	Sach and Heizmann (2001)
Langenau 1	Proboscidea	*Gomphotherium angustidens*	Sach and Heizmann

Locality	Supraspecific taxa	Species	References
			(2001)
Langenau 1	Rhinocerotidae	cf. *Brachypotherium brachypus*	Sach and Heizmann (2001)
Langenau 1	Equidae	*Anchitherium aurelianense*	Sach and Heizmann (2001)
Langenau 2	Palaeomerycidae	*Palaeomeryx* sp.	Sach and Heizmann (2001)
Langenau 1	Cervidae	*Heteroprox larteti*	Böhme et al. (2012a)

81

82 **Gerlenhofen**

83 Age: ~17 Ma (Aiglstorfer et al., 2014b)

84 Taxa:

Locality	Supraspecific taxa	Species	References
Gerlenhofen	Proboscidea	*Gomphotherium* cf. *angustidens*	Sach and Heizmann (2001)
Gerlenhofen	Rhinocerotidae	*Brachypotherium brachypus*	Sach and Heizmann (2001)

85

86 **Sandelzhausen**

87 Age: 16.58–16.37 Ma (Böhme et al., 2011)

88 Taxa:

Locality	Supraspecific taxa	Species	References
Sandelzhausen	Proboscidea	*Zygolophodon turicensis*	Göhlich (2010)
Sandelzhausen	Equidae	*Anchitherium aurelianense*	Kaiser (2009)
Sandelzhausen	Palaeomerycidae	*Germanomeryx fahlbushi*	Rössner (2010)

89

90 **Häder**

91 Age: ~16,2 Ma (Böhme et al., 2012a)

92 Taxa:

Locality	Supraspecific taxa	Species	References
Häder	Chalicotheriidae	*Anisodon grande*	Guérin 2012
Häder	Equidae	*Anchitherium aurelianense*	Eronen and Rössner (2007)
Häder	Cervidae	*Heteroprox larteti*	Eronen and Rössner (2007)

93

94 **Heggbach**

95   Age: ~16 Ma (Aiglstorfer et al., 2014b)

96   Taxa:

Locality	Supraspecific taxa	Species	References
Heggbach	Proboscidea	*Gomphotherium angustidens*	Bechly and Sach (2002)
Heggbach	Equidae	*Anchitherium aurelianense*	Bechly and Sach (2002)
Heggbach	Palaeomerycidae	*Palaeomeryx kaupi*	Bechly and Sach (2002)
Heggbach	Cervidae	*Heteroprox larteti*	Böhme et al. (2012a)
Heggbach	Carnivora	*Amphicyon major*	Bechly and Sach (2002)

97

98   **Stätzling**

99   Age: ~14.8 Ma (Aiglstorfer et al., 2014b)

100   Taxa:

Locality	Supraspecific taxa	Species	References
Stätzling	Rhinocerotidae	*Brachypotherium brachypus*	Eronen and Rössner (2007)
Stätzling	Chalicotheriidae	*Anisodon grande*	Eronen and Rössner (2007)
Stätzling	Equidae	*Anchitherium aurelianense*	Eronen and Rössner (2007)
Stätzling	Palaeomerycidae	*Palaeomeryx eminens*	Eronen and Rössner (2007)
Stätzling	Cervidae	*Heteroprox larteti*	Böhme et al. (2012a)

101

102   **Friedberg**

103   Age: ~14.2 (Böhme et al., 2012a)

104   Taxa:

Locality	Supraspecific taxa	Species	References
Friedberg	Rhinocerotidae	*Brachypotherium brachypus*	Eronen and Rössner (2007)

105

106   **Steinheim**

107   Age: ~13.5 Ma (Tütken et al., 2006)

108   Taxa:

Locality	Supraspecific taxa	Species	References
Steinheim	Rhinocerotidae	*Brachypotherium brachypus*	Tütken et al. (2006)
Steinheim	Equidae	*Anchitherium aurelianense*	Tütken et al. (2006)
Steinheim	Palaeomerycidae	*Palaeomeryx eminens*	Tütken et al. (2006)

Steinheim	Cervidae	*Heteroprox larteti*	Böhme et al. (2012a)

109

Massenhausen

111   Age: ~12.6 Ma (Böhme, 2012a)

112   Taxa:

Locality	Supraspecific taxa	Species	References
Massenhausen	Rhinocerotidae	*Hoploaceratherium tetradactylum*	Eronen and Rössner (2007)
Massenhausen	Rhinocerotidae	*Brachypotherium brachypus*	Eronen and Rössner (2007)
Massenhausen	Chalicotheriidae	*Anisodon grande*	Eronen and Rössner (2007)
Massenhausen	Equidae	*Anchitherium aurelianense*	Eronen and Rössner (2007)

113

Hammerschmiede

115   Age: 11.62–11.0 Ma (Böhme et al., 2008, 2019)

116

117   Taxa:

Locality	Supraspecific taxa	Species	References
Hammerschmiede	Rhinocerotidae	*Hoploaceratherium belvederense*	Kirscher et al. (2016)
Hammerschmiede	Chalicotheriidae	*Anisodon grande*	Kirscher et al. (2016)

118

Atzelsdorf

120   Age: ~11.1 Ma (Aiglstorfer et al., 2014b)

121

122   Taxa:

Locality	Supraspecific taxa	Species	References
Atzelsdorf	Equidae	*Anchitherium aurelianense*	Hillenbrand et al. (2009)
Atzelsdorf	Palaeomerycidae	*Palaeomeryx eminens*	Hillenbrand et al. (2009)

123

124

References

126   Aiglstorfer, M., Bocherens, H., Böhme M., 2014a. Large Mammal Ecology in the late Middle

127   Miocene lokality Gratkorn (Austria). Paleodivers. Paleoenv. 94, 189–213.

128   https://doi.org/10.1007/s12549-013-0145-5

129   Aiglstorfer, M., Rössner, G.E., Böhme, M., 2014b. *Dorcatherium naui* and pecoran ruminants

130   from the late Middle Miocene Gratkorn locality (Austria). The Sarmatian vertebrate

131   lokality Gratkorn, StyrianBasin. Paleodivers. Paleoenv. 94, 83–123.

132   https://doi.org/10.1007/s12549-013-0141-9

133   Astibia, H. 2012. Les Palaeomerycidae (Artiodactyla) de Sansan. In: Peigné, S., Sen, S.

134   (Eds.), Mammifères de Sansan. Mem. Mus. Natl. Hist. Nat. 203, 221–224.

135   Bechly, G., Sach, V.J., 2002. An interesting new fossil dragonfly (Anisoptera: Libellulidae:

136   "Brachydiplacini") from the Miocene of Germany, with a discussion on the phylogeny of

137   Tetrathemistinae and a fossil list for the lokality. Heggbach 325, 1–11.

138   Böhme, M, Ilg, A., Winklhofer, M., 2008. Late Miocene "washhouse" climate in Europe.

139   Earth Planet. Sci. Lett. 275, 393–401. https://doi.org/10.1016/j.epsl.2008.09.011

140   Böhme, M., Winklhofer, M., Ilg A., 2011. Miocene precipitation in Europe: Temporal trends

141   and spatial gradients. Palaeogeogr. Palaeoclim. Palaeoecol. 304, 212–218.

142   https://doi.org/10.1016/j.palaeo.2010.09.028

143   Böhme, M., Aiglstorfer, M., Uhl, D., Kullmer, O., 2012a. The antiquity of the Rhine River:

144   stratigraphic coverage of the Dinotheriensande (Eppelsheim Formation) of the Mainz

145   Basin (Germany). PLoS One 7, e36817. https://doi.org/10.1371/journal.pone.0036817

146   Böhme, M., Vasilyan, D., Winklhofer, M., 2012b. Habitat tracking, range dynamics and

147   palaeoclimatic significance of Eurasian giant salamanders (Cryptobranchidae) –indications

148   for elevated Central Asian humidity during Cenozoic global warm periods. Palaeogeogr.

149   Palaeoclim. Palaeoecol. 342/343, 64–72. https://doi.org/10.1016/j.palaeo.2012.04.032

150   Böhme, M., Spassov, N., Fuss, J., Tröscher, A., Deane, A. S., Prieto, J., Kirscher, U.,

151   Lechner, T., Begun, D.R., 2019. A new Miocene ape and locomotion in the ancestor of

152   great apes and humans. Nature 575, 489–493. https://doi.org/10.1038/s41586-019-1731-0

153   Bollinger, T.H., 1992. Kleinsäugerstratigraphie der miozänen Hörnlischüttung (Ostschweiz).

154   Documentanaturae 75, 1–296.

155   Daxner-Höck, P.M., Miklas-Tempfer, U.B., Göhlich, K., Hüttunen, E., Kazar, D., Nagel,

156   G.E., Roessner, O., Schultz, Ziegler, R., 2004. Marine and terrestrial vertebrates from the

157   Middle Miocene of Grund (Lower Austria). Geol. Carpath. 55, 191–197.

158   Engesser, B., 1972. Die obermiozäne Säugetierfauna von Anwil (Baselland). Tätigk.

159   Naturforsche. Ges. Baselland 28, 35–363.

160   Eronen, J.T., Rössner, G.E., 2007. Wetland Paradise Lost: Miocene Community Dynamics in

161   Large Herbivore Mammals from the German Molasse Basin. Evol. Ecol. Res. 9, 471–

162   494.

163   Fejfar, O., 1990. The Neogene vertebrate paleontology sites of Czechoslovakia: A

164   contribution to the Neogene terrestric biostratigraphy of Europe based on rodents, in:

165   Lindsay, E.H., Fahlbusch, V., Mein P. (Eds.), Proceedings of a NATO Advances Research

166   Workshop on European Neogene Mammal Chronology. Plenum Press, New York, pp.

167   211–236.

168   Heissig, K., 2012. Les Rhinocerotidae (Perissodactyla) de Sansan. In: Peigné, S., Sen, S.

169   (Eds.), Mammifères de Sansan. Mem. Mus. Natl. Hist. Nat. 203, 317–485.

170   Hillenbrand, V., Göhlich U.B., Rössner, G.E., 2009. The early Vallesian vertebrates of

171   Atzelsdorf (Late Miocene, Austria). Ruminantia. Ann. Naturhist. Mus. Wien 111 A, 519–

172   556.

173   Gross, M., Böhme, M., Havlik, P., Aiglstorfer, M., 2014. The late Middle Miocene

174   (Sarmatian s.str.) fossil site Gratkorn – the first decade of research, geology, stratigraphy

175   and vertebrate fauna. Paleodivers. Paleoenv. 94, 5–20.

176   https://doi.org/10.1007/s12549-013-0149-1

177   Göhlich U.B., 2010. The Proboscidea (Mammalia) from the Miocene of Sandelzhausen

178   (southern Germany). Paläontolo. Z. 84, 163–204.

179   https://doi.org/10.1007/s12542-010-0053-1

180   Guérin C., 2012. *Anisodon grande* (Perissodactyla, Chalicotheriidae) de Sansan. In: Peigné,

181   S., Sen, S. (Eds.), Mammifères de Sansan. Mem. Mus. Natl. Hist. Nat. 203, 279–315.

182   Harzhauser, M., Neubauer, T.A., 2018. Opole (Poland) – a key locality for middle Miocene

183   terrestrial mollusc faunas. Bull. Geosci. 93, 71–146.

184   https://doi.org/10.3140/bull.geosci.1692

185   Heissig, K., 2005. The fossil rhinoceroses of Rudabánya. Palaeontogr. Ital. 90, 217–2158.

186   Hyžný, M., Hudáčková, N., Biskupič, R., Rybár, S., Fuksi, T., Halásová, E., Zágoršek, K.,

187   Jamrich, J., Ledvák, P., 2012. Devínska Kobyla – a window into the Middle Miocene

188   shallow-water marine environments of the Central Paratethys (Vienna Basin, Slovakia).

189   Acta Geol. Slovaca 4, 95–111.

190   Ivanov, M., in press. Miocene snakes of Eurasia - a review of the evolution of snake

191   communities, in: D. Gower and H. Zaher (eds.), A Contribution to the Origin and Early

192   Evolution of Snakes, Systematics Association Special Volume Series, Cambridge

193   University Press.

194   Kaiser, T.M., 2009. *Anchitherium aurelianense* (Equidae, Mammalia): a brachydont ''dirty

195   browser'' in the community of herbivorous large mammals from Sandelzhausen (Miocene,

196   Germany). Paläontol. Z. 83, 131–140.

197   https://doi.org/10.1007/s12542-009-0002-z

198   Kirscher, T., Prieto, J., Bachtadse, V., Abdul Aziz, H., Doppler, G., Hagmaier, M., Böhme

199   M., 2016. A biochronologic tie-point for the base of the Tortonian stage in European

200   terrestrial settings: Magnetostratigraphy of the topmost Upper Freshwater Molasse

201   sediments of the North Alpine Foreland Basin in Bavaria (Germany). Newsl. Stratigr. 49,

202   445–467. https://doi.org/10.1127/nos/2016/0288

203   Kowalski, K., 1990. Stratigraphy of Neogene mammals in Poland, in: Lindsay, E.H.,

204   Fahlbusch, V., Mein, P. (Eds.), European Neogene Mammal Chronology. Plenum Press,

205   New York, pp. 193–209.

206   Pickford, M., Laurent, Y., 2014. Valorisation of palaeontological collections: nomination of a

207   lectotype for *Conohyus simorrensis* (Lartet, 1851), Villefranche d'Astarac, France, and

208   description of a new genus of tetraconodont. Estud. Geol. 70, 1–28.

209   http://dx.doi.org/10.3989/egeol.41261.262

210   Rössner, G., 2010. Systematics and palaeoecology of Ruminantia (Artiodactyla, Mammalia)

211   from the Miocene of Sandelzhausen (southern Germany, Northern Alpine Foreland Basin).

212   Paläontol. Z. 84, 123–162. https://doi.org/10.1007/s12542-010-0052-2

213   Sabol, M., Holec, P., 2002. Temporal and spatial distribution of Miocene mammals in the

214   Western Carpathians. Geol. Carpath. 53, 269–279.

215   Sabol, M., Kovac, M., 2006. Badenian Palaeoenvironment, Faunal Succession and

216   Biostratigraphy: A Case Study from Northern Vienna Basin, Devinska Nova Ves-Bonanza

217   site (Western Carpathians, Slovakia). Beitr. Palaont. 30, 415–425.

218   Sach, V.J., Heizmann, E.P.J., 2001. Stratigraphy and mammal faunas of the Brackwasser

219   molasse in the surroundings of Ulm (Southwest Germany). Stuttg. Beitr. Naturk Serie B,

220   310, 1–95.

221   Thenius, E. 1948. Zur Kenntnis der fossilen Hirsche des Wiener Beckens, unter besonderer

222   Berücksichtigung ihrer stratigraphischen Bedeutung. Ann. Nat. Hist. Mus. Wien. 56, 262–

223   308.

224   Thenius, E. 1951. *Gazella* cf. *deperdita* aus dem mitteleuropäischen Vindobonien und das

225   Auftreten der Hipparionfauna. Eclogae Geol. Helv. 44, 381–394.

226   Thenius, E., 1959. Wirbeltierfaunen, in: Lotze, F. (Ed.), Handbuch der Stratigraphischen

227   Geologie, III Band 2. Teil, Papp, A., Thenius, E., Tertiär. Ferdinand Enke Verlag,

228   Stuttgart, 328 pp.

229   Tütken, T., Vennemann. T.W., Janz, H., Heizmann, E.P.J., 2006. Palaeoenvironment and

230   palaeoclimate of the Middle Miocene lake in the Steinheim basin, SW Germany: A

231   reconstruction from C, O, and Sr isotopes of fossil remains. Palaeogeogr. Palaeoclimatol.

232   Palaeoecol. 241, 457–491. https://doi.org/10.1016/j.palaeo.2006.04.007

233   Van der Made, J., 2012. *Eotragus clavatus* (Artiodactyla, Bovidae, Boselaphini) de Sansan,

234   in: Peigné, S., Sen S. (Eds), Mammifères de Sansan. Mém. Mus. Nat. Hist. Natl. 203, 145–

235   199.

Supplementary Table 1

List of studied material with distribution of skeletal elements for each determined taxa.

			MINIMAL NUMBER OF ELEMENTS (MNE)			SKULL				UPPER DENTITION							LOWER DENT		
Supraspecific taxa	Species	Institution	Specimens	Rounded bones	Fresh bones	Skull bones	Antler/Horn	Upper jaw	Lower jaw	I2	C	P3	P4	M1	M2	M3	d4	p2	p3
Proboscidea	*Prodeinotherium bavaricum*	MZM	1	0	1											1			
Proboscidea	*Zygolophodon turicensis*	MZM, IPUW[2], RMM[3]	70	2	68			2	4, 1[2]	27, 1[3]			1	5	7, 1[2]	5, 2[2]	1		
Proboscidea	*Gomphotherium angustidens*	MZM	4	0	4			1		1					2				
Rhinocerotidae	*Hoploaceratherium* sp.	MZM	17	0	17														
Rhinocerotidae	*Brachypotherium brachypus*	MZM, IPUW[2], RMM[3]	24	1	23			1	2, 1[2], 1[3]	1			1	1	2	1		1	1
Chalicotheriidae	*Anisodon grande*	MZM	3	0	3														
Equidae	*Anchitherium* sp.	MZM	3	1	2			1											
Palaeomerycidae	Palaeomerycidae indet.	MZM, IPUW[2]	14	2	12				2										
Cervidae	*Heteroprox larteti*	MZM	3	2	1		3												
Bovidae	*Tethytragus stehlini*	MZM, IPUW[2]	20	7	13	1	11, 2[2]	2	4										
Suidae	*Retroporcus matritensis*	RMM[3]	1	0	1				1[3]										
Carnivora	*Amphicyon* cf. *major*	MZM, ÚGV[1]	3	1	2						1, 1[1]								
Testudinidae	*Testudo kalksburgensis*	MZM	8	0	8														
Trionychidae	Trionychidae indet.	IPUW[2]	1	1	0														
Cervidae/Bovidae	Undetermined	MZM, IPUW[2]	11	4	7														
Proboscidea	Undetermined	MZM, IPUW[2]	190	20	170	2													
Rhinocerotidae	Undetermined	MZM, IPUW[2]	34	1	33	1			3										
Testudines	Undetermined fragments	MZM, IPUW[2]	57	14	43														
TOTAL (MNE)			**464**	**56**	**408**	**4**	**16**	**6**	**20**	**30**	**2**	**1**	**2**	**7**	**11**	**10**	**1**	**1**	**1**

1 = Department of Geological Sciences, Faculty of Sciences, Masaryk University (ÚGV)

2 = Paleontological Institut University Vienna (IPUW)

3 = Regional Museum in Mikulov (RMM)